Efficient Zirconocene-Coupling of Silicon-Substituted Diynes to Polymers and Macrocycles

Shane S. H. Mao, Feng-Quan Liu, and T. Don Tilley*

Contribution from the Department of Chemistry, University of California at Berkeley, Berkeley, California 94720-1460

Received September 10, 1997

Abstract: The zirconocene-coupling of diynes with internal silicon substituents, $MeC{\equiv}CMe_2SiArSiMe_2C{\equiv}CMe$ (**1**: Ar = 1,4-C_6H_4; **2**: Ar = 1,3-C_6H_4; **3**: Ar = 4,4′-$C_6H_4C_6H_4$), generates regiospecific polymers containing zirconacyclopentadiene in the main chain (**5**−**7**). These organometallic polymers hydrolyze cleanly to butadienediyl polymers of the type $[Me_2SiArSiMe_2CH{=}CMeCMe{=}CH]_n$ (**11**−**13**), and polymer **5** reacts with iodine to give the iodine-containing polymer [1,4-$Me_2SiC_6H_4SiMe_2C(I){=}CMeCMe{=}C(I)]_n$ (**14**). The organometallic polymers undergo facile and high-yield degradations to macrocycles under mild conditions (refluxing tetrahydrofuran solution). The size and shape of the resulting macrocycles depend upon the nature of the diyne spacer group. Thus, polymers **5** and **7** containing parallel diyne units convert to the trimeric macrocycles $[Me_2SiArSiMe_2C_4Me_2ZrCp_2]_3$ (**15**: Ar = 1,4-C_6H_4; **24**: Ar = 4,4′-$C_6H_4C_6H_4$), while polymer **6** gives the dimeric macrocycle [1,3-$Me_2SiC_6H_4SiMe_2C_4Me_2ZrCp_2]_2$ (**18**). The dimeric macrocycle $[Me_2SiC_6H_4SiMe_2C_6H_4SiMe_2C_4Me_2ZrCp_2]_2$ (**20**) was obtained directly from the zirconocene coupling of $Me_2Si[(1,4\text{-}C_6H_4)SiMe_2(C{\equiv}CMe)]_2$ (**4**) by heating the reaction mixture to reflux. In a similar manner, the diyne $Me_2Si(C{\equiv}CMe)_2$ was converted in high yield to the hexameric macrocycle $[Me_2SiC_4Me_2ZrCp_2]_6$ (**22**). The macrocycles **15**, [1,4-$Me_2SiC_6H_4SiMe_2C_4Me_2H_2]_3$ (**16**), and **18** were characterized by single-crystal X-ray crystallography. Molecules of **15** adopt a nearly planar C_3 macrocyclic structure with a cavity described by an average transannular Si···Si distance of 13.2 Å, while the hydrolyzed macrocycle **16** has a chair conformation. This conformation change results from conversion of cis diene groups in the zirconacyclopendiene fragments to trans diene groups in **16**. The high-yield formation of macrocycles apparently results from the reversible nature of the alkyne-coupling reaction, which allows for a low-energy pathway to the smallest macrocycle possessing minimal ring strain.

Major synthetic efforts in materials and supramolecular chemistry target the assembly of polymers, oligomers, and macrocycles with well-defined structures and novel properties. Much of this chemistry is based on transition metal-mediated coupling reactions, primarily with palladium reagents.[1] Our group has been exploring organometallic pathways to macromolecular structures and in particular ones that incorporate transition metal fragments.[2,3] New classes of metal-containing macromolecules have attracted considerable attention because of the wide range of magnetic, electrical, optical, and catalytic properties that are associated with transition metal centers.[4] In addition, stoichiometric reactions involving these metal centers may provide useful means for chemically modifying the materials of interest.

Over the past two decades, zirconacyclopentadienes have been studied intensively as synthetic intermediates in organic synthesis.[5−7] These versatile synthons are readily converted to other derivatives including dienes,[5] aromatics,[6] and heterocycles[7]

---

[1] (a) Tour, J. M. *Chem. Rev.* **1996**, *96*, 537. (b) Tsuji, J. *Palladium Reagents and Catalysts − Innovations in Organic Synthesis;* John Wiley and Sons: New York, 1995. For further examples and leading references, see: (c) Goldfinger, M. B.; Swager, T. M. *J. Am. Chem. Soc.* **1994**, *116*, 7895. (d) McClain, M. D.; Whittington, D. A.; Mitchell, D. J.; Curtis, M. D. *J. Am. Chem. Soc.* **1995**, *117*, 3887. (e) Delnoye, D. A. P.; Sijbesma, R. P.; Vekemans, J. A. J. M.; Meijer, E. W. *J. Am. Chem. Soc.* **1996**, *118*, 8717. (f) Ma, L.; Hu, Q.-S.; Vitharana, D.; Wu, C.; Kwan, C. M. S.; Pu, L. *Macromolecules* **1997**, *30*, 204. (g) Kumar, A.; Reynolds, J. R. *Macromolecules* **1996**, *29*, 7629. (h) Anthony, J.; Boudon, C.; Diederich, F.; Gisselbrecht, J.-P.; Gramlich, V.; Gross, M.; Hobi, M.; Seiler, P. *Angew. Chem., Int. Ed. Engl.* **1994**, *33*, 763.

[2] (a) Mao, S. S. H.; Tilley, T. D. *J. Am. Chem. Soc.* **1995**, *117*, 5365. (b) Mao, S. S. H.; Tilley, T. D. *J. Am. Chem. Soc.* **1995**, *117*, 7031. (c) Mao, S. S. H.; Tilley, T. D. *Macromolecules* **1996**, *29*, 6362. (d) Mao, S. S. H.; Tilley, T. D. *J. Organomet. Chem.* **1996**, *521,* 425. (e) Mao, S. S. H.; Tilley, T. D. *Macromolecules* **1997**, *30*, 5566.

[3] Buretea; M. A.; Tilley; T. D. *Organometallics* **1997**, *16*, 1507.

[4] Selected references for metal-containing polymers: (a) *Inorganic and Organometallic Polymers II;* ACS Symposium Series 572, Wisian-Nielson, P., Allcock, H. R., Wynne, K. J., Eds.; American Chemical Society: Washington, D.C., 1994. (b) Oriol, L.; Serrano, J. L. *Adv. Mater.* **1995**, *7*, 348. (c) *Metal Containing Polymer Systems*; Sheats, J. E., Carraher, C. E., Pittman, C. U., Eds.; Plenum: New York, 1985. (d) Manners, I. *Angew. Chem., Int. Ed. Engl.* **1996**, *35*, 1603. (e) Rosenblum, M.; Nugent, H. M.; Jang, K. S.; Labes, M. M.; Cahalane, W.; Klemarczyk, P.; Reiff, W. M. *Macromolecules* **1995**, *28*, 6330. (f) Altmann, M.; Bunz, U. H. F. *Angew. Chem., Int. Ed. Engl.* **1995**, *34*, 569. (g) Stanton, C. E.; Lee, T. R.; Grubbs, R. H.; Lewis, N. S.; Pudelski, J. K.; Callstrom, M. R.; Erickson, M. S.; McLaughlin, M. L. *Macromolecules* **1995**, *28,* 8713. (h) Zhu, S. S.; Swager, T. M. *Adv. Mater.* **1996**, *8*, 497. (i) Chisholm, M. H. *Angew. Chem., Int. Ed. Engl.* **1991**, *30*, 673. (j) Peng, Z.; Yu, L. *J. Am. Chem. Soc.* **1996**, *118*, 3777. (k) Pollagi, T. P.; Geib, S. J.; Hopkins, M. D. *J. Am. Chem. Soc.* **1994**, *116*, 6051. (l) *Metal-Containing Polymeric Materials*; Pittman, C. U., Jr., Carraher, C. E., Zeldin, M., Sheats, J. E., Culbertson, B. M., Eds., Plenum: New York, 1996.

[5] (a) Broene, R. D.; Buchwald, S. L. *Science* **1993**, *261*, 1696. (b) Negishi, E.; Takahashi T. *Acc. Chem. Res* **1994**, *27*, 124. (c) Cardin, D. J.; Lappert, M. F.; Raston, C. L. *Chemistry of Organozirconium and Hafnium Compounds*; John Wiley & Sons: New York, 1986. (d) Buchwald, S. L.; Nielsen, R. B. *J. Am. Chem. Soc.* **1989**, *111*, 2870. (e) Ashe, A. J.; Kampf, J. W. *J. Am. Chem. Soc.* **1992**, *114*, 372.

[6] Takahashi, T.; Kotora, M.; Xi, Z. F. *J. Chem. Soc., Chem. Commun.* **1995**, 361.

S0002-7863(97)03180-6 CCC: $15.00

and are readily formed by the coupling of alkynes by "zirconocene", which may be generated in solution as a reactive intermediate.[8] Negishi has described a simple procedure for the generation of zirconocene,[8a] stabilized as a 1-butene adduct,[8e] by addition of 2 equiv of ^nBuLi to a THF solution of Cp_2ZrCl_2 at −78 °C. The addition of alkynes to zirconocene generated by this method produces zirconacyclopentadienes in high yields. We envisioned use of this powerful carbon−carbon bond-forming reaction in the construction of macromolecules with novel structures (eq 1). It was thought that such polymers might exhibit unusual electronic properties and serve as synthetic precursors to a wide range of alternating copolymers. With this approach, we have obtained polymers containing macrocyclic rings in the main chain[2c] and π-conjugated polymers with all-carbon backbones.[2e] In related work, two groups have reported the synthesis of cobaltacyclopentadiene polymers by a similar strategy.[9]

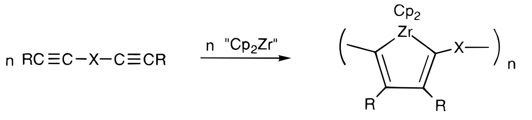

(1)

To control the regiochemistry of the zirconocene-coupling reactions we also investigated the coupling of diynes with silicon substituents, since it is known that alkynyl silanes are coupled exclusively to α-silyl-substituted zirconacyclopentadienes.[10] Part of this work, which involved the coupling of $MeC{\equiv}CSiMe_2C_6H_4SiMe_2C{\equiv}CMe$ to the stereoregular polymer $[Me_2SiC_6H_4SiMe_2C_4Me_2ZrCp_2]_n$, has been communicated.[2a] To our surprise, we found that this polymer readily and quantitatively degraded upon gentle heating to the macrocyclic trimer $[Me_2SiC_6H_4SiMe_2C_4Me_2ZrCp_2]_3$. This simple, high-yield route to a functionalized macrocycle is remarkable in that syntheses of macrocycles are generally associated with multiple steps, difficult separations, and low yields. Given the demonstrated potential for the zirconocene-coupling of diynes to produce new polymers and macrocycles, we have embarked on a systematic study to explore the limitations and possibilities of this method. With respect to macrocycle syntheses, we wish to explore its potential for producing cyclic species with various sizes, shapes, and functionalities. In this regard, we report here the synthesis of polymers and macrocycles via the zirconocene-coupling of diynes that incorporate $-SiMe_2(aryl)_xSiMe_2-$ and $-SiMe_2-$ spacer groups.

Results

Synthesis of Diynes. Diynes 1,4-$MeC{\equiv}C(Me_2Si)C_6H_4(SiMe_2)C{\equiv}CMe$ (**1**), 1,3-$MeC{\equiv}C(Me_2Si)C_6H_4(SiMe_2)C{\equiv}CMe$ (**2**), and 4,4′-$MeC{\equiv}C(Me_2Si)C_6H_4C_6H_4(SiMe_2)C{\equiv}CMe$ (**3**) were synthesized in three steps. First, the appropriate dibromoarenes were coupled with $(EtO)_2SiMe_2$ to afford silyl ethers of the type $(EtO)Me_2Si{-}Ar{-}SiMe_2(OEt)$ in moderate yields (55−65%).[11] Subsequent conversion of the silyl ethers to the corresponding silyl chlorides is nearly quantitative,[11] and reactions of the silyl chlorides with lithium propylide lead to diynes **1**−**3** in overall yields of 60%, 53%, and 48%, respectively. Note that direct reactions of the $(EtO)Me_2Si{-}Ar{-}SiMe_2(OEt)$ compounds with $LiC{\equiv}CMe$ gave little or no product, even under forcing conditions. The diyne $Me_2Si[C_6H_4SiMe_2(C{\equiv}CMe)]_2$ (**4**) was obtained in 82% yield by the reaction of Me_2SiCl_2 with $LiC_6H_4SiMe_2C{\equiv}CMe$.

Synthesis of Zirconocene-Containing Polymers. Generation of a slight excess of "zirconocene" (by addition of 2 equiv of ^nBuLi to zirconocene dichloride at −78 °C, and then warming to room temperature)[8a] in the presence of diynes **1**−**3** afforded the zirconocene polymers **5**−**7**, respectively (Scheme 1). Crude polymers were extracted into benzene or toluene and then precipitated with a large amount of pentane to give yellow powders in 50−90% yield. These polymers are reasonably pure by NMR spectroscopy and elemental analysis.

Isolated polymer **5** exhibited the molecular weight distribution shown in Figure 1a (by gel permeation chromatography, GPC), with $M_w/M_n = 13\,000/4600$ (vs polystyrene standards). This polymer is soluble in most organic solvents, and thin films are readily cast from THF solutions. The solid polymer is sensitive to moisture but relatively stable in dry air.

To help elucidate the structure of polymer **5**, the model zirconacyclopentadiene compound $Cp_2ZrC_4(SiMe_2Ph)_2Me_2$ (**8**) was synthesized, via the zirconocene-coupling of $PhMe_2SiC{\equiv}CMe$. Compound **8** is the only organometallic product from this reaction. Its ^1H NMR spectrum exhibits three singlets at δ 0.29, 1.74, and 6.06, assigned to resonances for the silylmethyl, dienyl methyl, and cyclopentadienyl protons, respectively (Figure 2). On the basis of NMR data for **8** and its hydrolysis product, complex **8** possesses a 2,5-bis(silyl)-substituted metallacycle ring. A similar compound, 2,5-bis(trimethylsilyl)-3,4-diphenylzirconacyclopentadiene, has been synthesized and crystallographically characterized.[10] In addition, the coupling of $Me_3SiC{\equiv}CCH_3$ by bis(cyclopentadienyl)hafnium produced 2,5-bis(trimethylsilyl)-3,4-dimethylhafnacyclopentadiene, also exhibiting Me_3Si groups at the α-positions.[12] This high regioselectivity has been attributed by Erker to a steric effect, which favors placement of the bulky $SiMe_3$ group in the least sterically hindered position.[10] This regiospecificity is also present in polymer **5**. As shown in Figure 2, the ^1H NMR spectrum of polymer **5** is almost identical with that for compound **8**, except that all of the peaks are slightly broad. This strongly supports the structural assignment for polymer **5**, with 2,5-bis(silyl)zirconacyclopentadiene repeat units in the main chain (Scheme 1).

Diyne **2**, which possesses a spacer group with a nonlinear geometry, was also coupled with zirconocene to afford a regiospecific polymer (**6**; 50% yield, $M_w/M_n = 5800/2600$). The lower molecular weight and yield of **6** (vs **5**) may be due to the shorter spacer group (1,3-C_6H_4 vs 1,4-C_6H_4), which may lead to less extensive coupling due to greater crowding at the reacting Zr centers. The chemical shifts in both the ^1H and ^{13}C NMR spectra of **6** are similar to those in polymer **5** and model compound **8** and are consistent with the structure indicated in

---

(7) Fagan, P. J.; Nugent, W. A.; Calabrese, J. C. *J. Am. Chem. Soc.* **1994**, *116*, 1880.

(8) (a) Negishi, E.; Cederbaum, F. E.; Takahashi, T. *Tetrahedron Lett.* **1986**, *27*, 2829. (b) Alt, H.; Rausch, M. D. *J. Am. Chem. Soc.* **1974**, *96*, 5936. (c) Demerseman, B.; Bouquet, G.; Bigorgne, M. *J. Organomet. Chem.* **1977**, *132*, 223. (d) Thanedar, S.; Farona, M. F. *J. Organomet. Chem.* **1982**, *235*, 65. (e) Buchwald, S. L.; Watson, B. T.; Huffman J. C. *J. Am. Chem. Soc.* **1987**, *109*, 2544.

(9) (a) Ohkubo, A.; Aramaki, K.; Nishihara, H. *Chem. Lett.* **1993**, 271. (b) Nishihara, H.; Shimura, T.; Ohkubo, A.; Matsuda, N.; Aramaki, K. *Adv. Mater.* **1993**, *5*, 752. (c) Nishihara, H.; Ohkubo, A.; Aramaki, K. *Synth. Met.* **1993**, *55*, 821. (d) Tomita, I.; Nishio, A.; Igarashi, T.; Endo, T. *Polym. Bull.* **1993**, *30*, 179. (e) Tomita, I.; Nishio, A.; Endo, T. *Macromolecules* **1994**, *27*, 7009.

(10) Erker, G.; Zwettler, R. *J. Organomet. Chem.* **1991**, *409*, 179. (b) Erker, G.; Zwettler, R.; Kruger, C.; Hyla-Kryspin, I.; Gleiter, R. *Organometallics* **1990**, *9*, 524. (c) Erker, G.; Zwettler, R.; Kruger, C.; Hyla-Kryspin, I.; Gleiter, R. *J. Organomet. Chem.* **1988**, *346*, C15.

(11) This method is slightly modified from that of a literature procedure. See: Nate, K.; Ishikawa, M.; Ni, H.; Watanabe, H.; Saheki, Y. *Organometallics* **1987**, *6*, 1673.

(12) Sabade, M. B.; Farona, M. F.; Zarate, E. A.; Youngs, W. J. *J. Organomet. Chem.* **1988**, *338*, 347.

Scheme 1

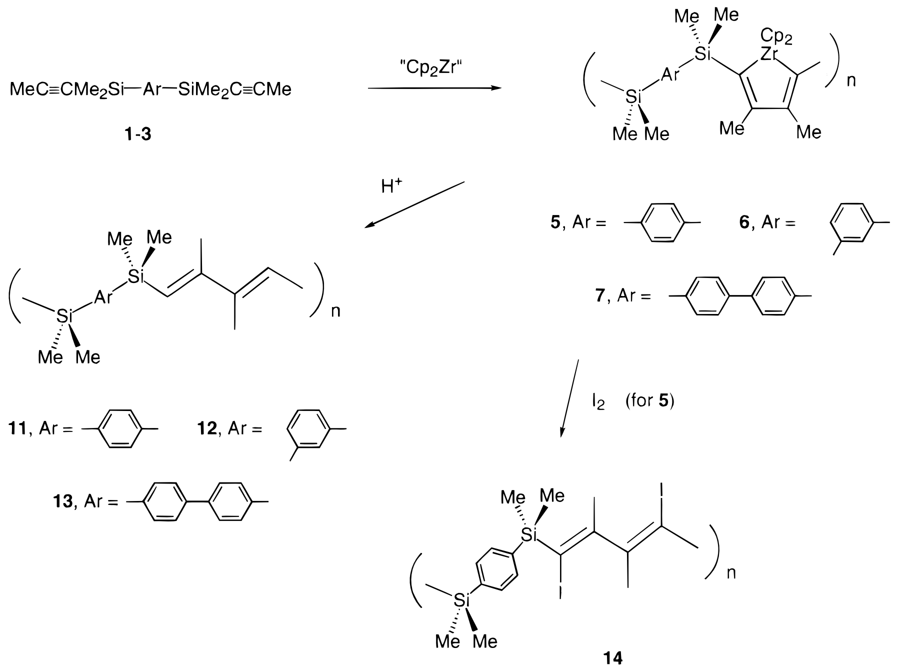

Scheme 1. Zirconocene-coupling of diyne **3** generated yellow polymer **7** (76% isolated yield; M_w/M_n = 18 000/8500), which exhibits ^1H and $^{13}C\{^1H\}$ NMR spectroscopic data that are closely related to those observed for polymers **5** and **6**.

End-group analysis of polymer **5** by ^1H NMR spectroscopy provided a number average molecular weight of ca. 28 000. The great disparity between this value and the molecular weight obtained by GPC (M_n = 4600) suggests that a significant fraction of the polymer chains have cyclic structures. This assumption was also supported by the lack of observable C≡C stretching vibrations in the IR spectrum. End group analysis of polymer **7** by ^1H NMR spectroscopy provided a molecular weight of ca. 10 000, which is close to the molecular weight (M_n) obtained by GPC (8500). This result may be attributed to the lesser tendency of this system to form cyclic structures (vide infra).

Reactions of Polymers 5−7. Zirconacyclopentadiene complexes are readily derivatized via reactions of the Zr−C bonds.[5−7] For example, compound **8** was quantitatively (by NMR spectroscopy) hydrolyzed to the diene $PhMe_2SiCH{=}CMeCMe{=}CHSiMe_2Ph$ (**9**), isolated as a crystalline solid in 87% yield. Compound **8** also reacted with iodine to give the corresponding diiododiene $PhMe_2SiC(I){=}CMeCMe{=}C(I)SiMe_2Ph$ (**10**) in 69% isolated yield. In contrast to **8** and **9**, compound **10** possesses inequivalent silylmethyl groups, as seen in the ^1H NMR spectrum by the presence of two singlets at δ 0.52 and 0.56, which do not coalesce to 90 °C in toluene-d_8. This inequivalence is presumably due to restricted rotation about the Si−C(I) bonds.

Metal-containing polymers **5**−**7** undergo reactions that are very similar to those described for compound **8** (Scheme 1). Hydrolysis of **5** (M_w/M_n = 13 000/4600) generated a colorless polymer **11** (M_w/M_n = 12 000/4200) in 94% isolated yield, with little or no degradation of the polymer backbone. The ^1H NMR spectrum of **11** contains the expected singlets at δ 0.42 (SiMe), 1.96 (=CMe), and 6.02 (=CH) and indicates the presence of only one type of observable repeat unit. The hydrolyses of **6** and **7** proceeded similarly, to give **12** and **13**. Reaction of **5** with iodine produced the vinyl iodide polymer **14** (M_w/M_n = 8800/5000) in 74% isolated yield. The NMR spectra for **14**

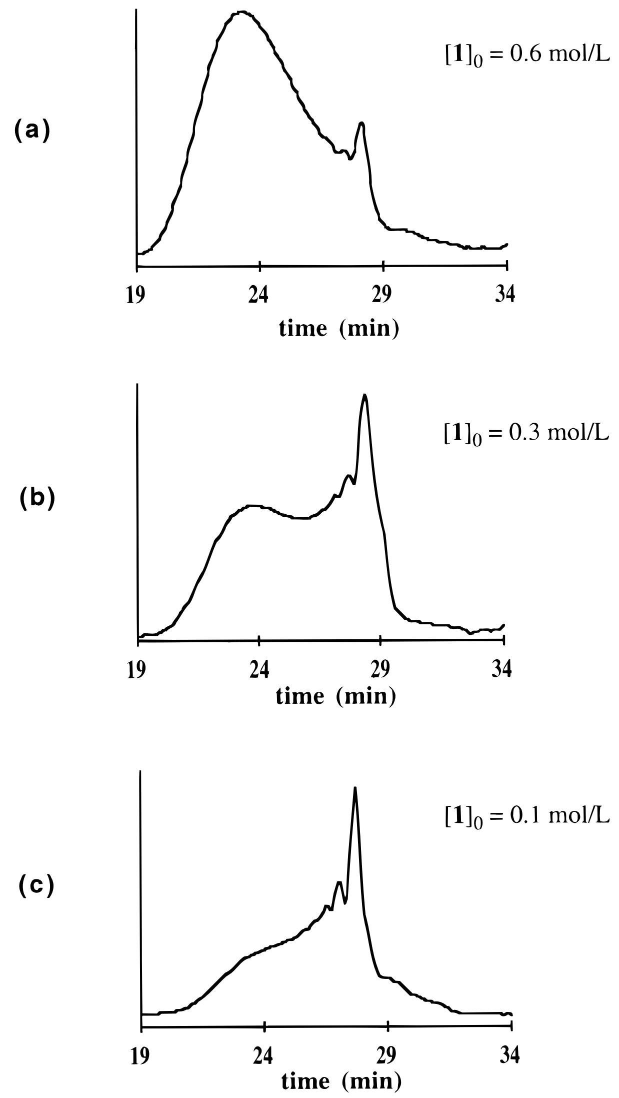

Figure 1. GPC traces of the zirconocene-coupling products obtained with different initial monomer concentrations.

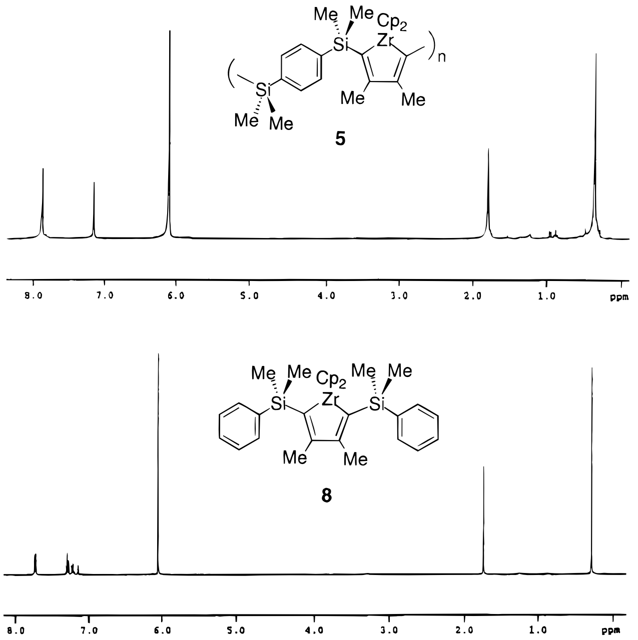

Figure 2. ^{1}H NMR spectra of polymer **5** and the model compound **8** (benzene-d_6 solvent).

are very similar to those for the model compound **10** and reveal the presence of inequivalent silylmethyl groups. Overall, the NMR spectra and the elemental analysis for fractionated **14** indicate the presence of a fairly regular structure.

Reactions of polymer **5** with $PhPCl_2$, S_2Cl_2, and $PhBCl_2$ did not provide clean conversions to well-defined polymers, and these reactions were in general accompanied by polymer degradations to low molecular weight species. Similar results were observed for reactions of these reagents with the model complex **8**.

The thermal stabilities of the polymers described above were investigated by thermogravimetric analysis (TGA). Thermally labile polymers **5**−**7** are characterized by initial weight losses at 90, 87, and 93 °C, respectively (under nitrogen). In contrast, the hydrolyzed polymers **11** and **13** are much more stable and reveal onset temperatures for decomposition at 435 and 426 °C, respectively. The DSC thermograms for **5**, **7**, **11**, and **13** reveal glass transition temperatures of −3.4, −4.0, 0.0, and −5.2 °C, respectively. Melting temperatures of 152 and 270 °C, respectively, were also observed for **11** and **13**. Interestingly, the DSC thermogram of **13** also exhibits two endothermic phase transitions at 86 and 115 °C.[13,14]

Polymer Degradations to Macrocycles. As shown in Figure 1a, the initially prepared sample of **5** has a primarily monomodal molecular weight distribution but a small sharp peak at a molecular weight value of ca. 1000 was also apparent. This peak suggested the favored production of a single cyclic species, and this possibility was tested by conducting the polymerization at lower monomer concentrations, which are expected to more greatly favor formation of cyclic species in a condensation polymerization.[15] As can be seen by Figure 1, the molecular weight distribution for **5** is strongly dependent on the initial monomer concentration. In particular, the peak at ca. 1000 amu appeared to correspond to a cyclic oligomer (**15**), since it increased in intensity under more dilute reaction conditions. In addition, the ratio of cyclic oligomer to polymer increased at elevated reaction temperatures. Refluxing **5** in benzene for 48 h afforded the macrocycle **15** in ca. 70% yield, along with low molecular weight species (at ca. $M_n = 400$, by GPC) and a substantial amount of white precipitate. In refluxing THF, polymer **5** degraded *quantitatively* (by GPC and NMR spectroscopy) to macrocycle **15** within 12 h (Figure 3 and Scheme 2). Thus, THF appears to accelerate this depolymerization reaction.

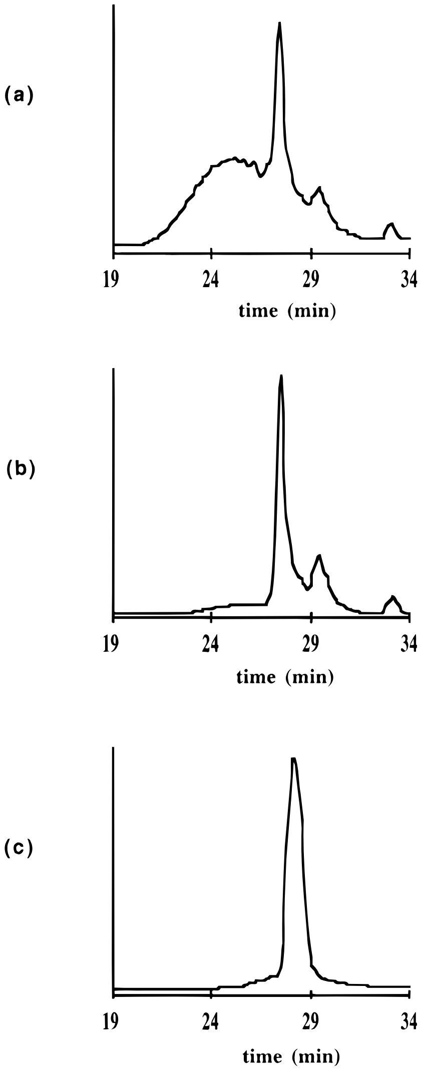

Figure 3. GPC traces for the thermal degradation products of polymer **5** in (a) refluxing benzene solution after 24 h, (b) refluxing benzene solution after 48 h, and (c) refluxing THF solution after 12 h.

The ^{1}H and ^{13}C NMR spectra of macrocycle **15** are very similar to those for polymer **5**, with only subtle differences in the chemical shifts. At room temperature, only one resonance for the silylmethyl protons was observed, but at −30 °C this resonance decoalesced into two separate peaks. This behavior signals the occurrence of a fluxional process, which is associated with an activation barrier of $\Delta G^{\ddagger} = 10.9(2)$ kcal/mol, as calculated from the Erying equation.[16] Addition of 6 equiv of

---

(13) (a) Cheng, S. Z. D.; Cao, M.-Y.; Wunderlich, B. *Macromolecules* **1986**, *19*, 1868. (b) Bassett, D. C.; Olley, R. H.; Al Raheil, I. A. M. *Polymer* **1988**, *29*, 1745.

(14) Hatakeyama, T.; Quinn, F. X. *Thermal Analysis: Fundamentals and Applications to Polymer Science;* Wiley: Chichester, 1994.

(15) (a) Allcock, H. R. *Contemporary Polymer Chemistry;* Prentice Hall, Englewood Cliffs, NJ, 1990.; Chapter 10, pp 232−257. (b) *Comprehensive Polymer Science;* Allen, G., Ed.; Pergamon: Oxford, England, 1989; Vol. 5, Chapter 6, pp 91−96. (c) Odian, G. *Principles of Polymerization*; John Wiley & Sons: New York, 1991; pp 73−77; 550−557. (d) Allen, P. E. M.; Patrick, C. R. *Kinetics and Mechanisms of Polymerization Reactions;* Wiley: New York, 1974; Chapter 5. (e) Odian, G. *Principles of Polymerization;* John Wiley & Sons: Staten Island, New York, 1991; pp 77−82.

Scheme 2

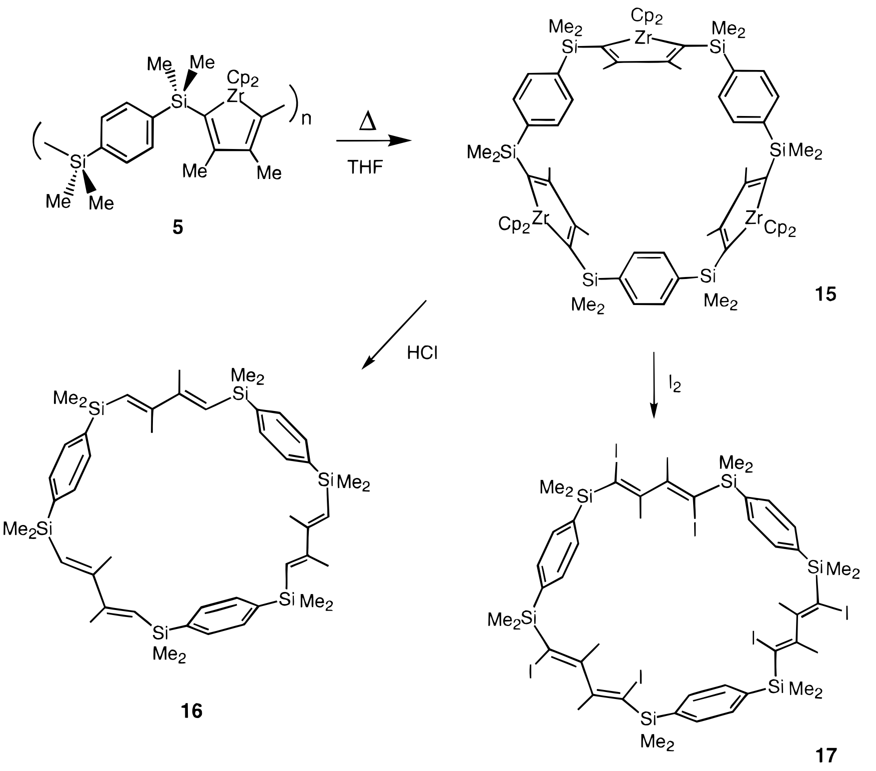

THF did not affect this fluxional behavior, which suggests that a mechanism involving metallacycle scission, as in polymer degradation, is unlikely. One possible mechanism is the rotation of the zirconacyclopentadiene units about the Si···Si axes, which moves the 6 Cp ligands from one side of the ring to the other. The most intense peaks in the mass spectrum of **15** correspond to the fragments $MeC{\equiv}CMe_2SiC_6H_4SiMe_2(C_4Me_2ZrCp_2)SiMe_2C_6H_4SiMe_2C{\equiv}CMe$ and $(Cp_2Zr)MeC{\equiv}CMe_2SiC_6H_4SiMe_2C{\equiv}CMe(ZrCp_2)$, which result from cleavage of the macrocyclic ring via rupture of the zirconacyclopentadiene units.

Macrocycle **15** is readily converted to other macrocycles via reactions of the Zr−C bonds. Hydrolysis of **15** with hydrochloric acid afforded cyclophane **16** in 98% yield (Scheme 2). The ^{1}H NMR and ^{13}C NMR spectra of **16** are very similar to those of hydrolyzed polymer **11**. Its trimeric nature was revealed by high-resolution mass spectroscopic studies and an X-ray crystal structure determination (vide infra). Reaction of **15** with iodine gave macrocycle **17** in 75% isolated yield. Interestingly, the ^{1}H and ^{13}C NMR spectra of **17** contain resonances for 4 inequivalent SiMe groups (presumably due to the presence of rotamers) which do not coalesce up to 90 °C. Similar to the vinyl iodide polymer **14**, these different isomers most likely arise from restricted rotations about the Si−C(I) bonds.

Air-sensitive, yellow crystals of **15** were grown from a THF/ether solution containing a slight amount of benzene. Crystallographic data are listed in Table 1, selected intramolecular distances and angles are listed in Table 2, and an ORTEP view of **15** is shown in Figure 4. These crystals contain 3.5 equiv of somewhat disordered benzene molecules per macrocycle, one of which is located near the center of the ring, in close contact with the dienyl methyl substituents. The trimeric ring is approximately planar, with five of the six Si atoms in a plane, and one displaced by 0.86 Å in the direction of the zirconocene groups, which all protrude from the same face of the ring and lie outside of the ring's perimeter. The slight bending in the ring appears to result merely from crystal-packing forces. The

Table 1. Crystallographic Data for **15**, **16**, and **18**

	compounds		
	15·$3.5C_6H_6$	**16**	**18**·2THF
	(a) Crystal Parameters		
empirical formula	$C_{99}H_{117}Si_6Zr_3$	$C_{24}H_{36}Si_3$	$C_{60}H_{80}O_2Si_4Zr_2$
formula weight	1749.21	408.8	1128.07
crystal system	monoclinic	monoclinic	triclinic
space group	$P2_1/n$	$P2_1/c$	$P\bar{1}$
a, Å	19.049(5)	7.3408(13)	9.5861(3)
b, Å	18.660(5)	10.9142(23)	10.5303(3)
c, Å	25.385(5)	31.789(6)	14.2562(4)
α, deg	90	90	93.546(1)
β, deg	90.074(19)	93.791(15)	103.243(1)
γ, deg	90	90	95.917(1)
volume, Å^3	9023.2(65)	2541.4(15)	1387.91(7)
Z	4	4	1
crystal color	yellow	colorless	yellow
ρ (calc), g cm^{-3}	1.29	1.07	1.35
temp, °C	−86	−128	−160
	(b) Data Collection		
diffractometer	Siemens P4	Siemens P4	Siemens Smart
monochromator		graphite	
radiation		Mo Kα ($\lambda = 0.71069$ Å)	
2θ range, deg	3−45	3−45	4−46.5
rflns collected	12206	3526	5643
indpt rflns	11755	3313	3892
std rflns	5520	1648	3495
	(c) Refinement[a]		
R(F), %	5.29[b]	9.77[b]	3.90[b]
R(wF), %	5.46	12.2	5.30
Δ/σ (max)	0.04	0.03	0.031
$\Delta(\rho)$, e Å^{-3}	0.54	0.40	0.52
GOF	1.28	2.85	2.17

[a] Quantity minimized = $\sum w\Delta;^2$ $R = \sum\Delta/\sum(F_o)$; $R(w) = \sum\Delta w^{1/2}/\sum(F_o{\cdot}w^{1/2})$, $\Delta = |(F_o - F_c)|$. [b] Quantity minimized = $R(wF^2) = \sum[w(F_o2 - F_c^2)^2]/S(wF_o2)^2]^{1/2}$; $R = \sum\Delta/\sum(F_o)$, $\Delta = |(F_o - F_c)|$.

---

(16) Lukehart, C. M. *Fundamental Transition Metal Organometallic Chemistry;* Brooks/Cole: Belmont, 1985; pp 196−210.

Table 2. Selected Intramolecular Distances and Angles for **15**

(a) Intramolecular Distances (Å)

Zr(1)−C(61)	2.255(10)	Si(1)−Si(4)	13.41(9)
Zr(1)−C(64)	2.238(10)	Si(2)−Si(5)	13.42(8)
Zr(2)−C(37)	2.252(11)	Si(3)−Si(6)	12.87(9)
Zr(2)−C(40)	2.247(9)	C(61)−C(62)	1.364(13)
Zr(3)−C(49)	2.245(10)	C(62)−C(63)	1.512(13)
Zr(3)−C(52)	2.244(10)	C(63)−C(64)	1.376(13)
Zr(1)−Cp(1)	2.230	C(37)−C(38)	1.363(13)
Zr(1)−Cp(2)	2.239	C(38)−C(39)	1.516(14)
Zr(2)−Cp(3)	2.234	C(39)−C(40)	1.348(13)
Zr(2)−Cp(4)	2.228	C(49)−C(50)	1.338(14)
Zr(3)−Cp(5)	2.212	C(50)−C(51)	1.503(14)
Zr(3)−Cp(6)	2.226	C(51)−C(52)	1.348(13)

(b) Bond Angles (Deg)

C(61)−Zr(1)−C(64)	82.4(4)	C(31)−Si(1)−C(64)	113.1(4)
C(37)−Zr(2)−C(40)	82.3(4)	C(34)−Si(2)−C(37)	111.1(5)
C(49)−Zr(3)−C(52)	80.4(4)	C(40)−Si(3)−C(43)	114.5(4)
Cp(1)−Zr(1)−Cp(2)	135.3	C(46)−Si(4)−C(49)	111.3(4)
Cp(3)−Zr(2)−Cp(4)	135.5	C(52)−Si(5)−C(55)	113.0(5)
Cp(5)−Zr(3)−Cp(6)	136.5	C(58)−Si(6)−C(61)	114.4(5)

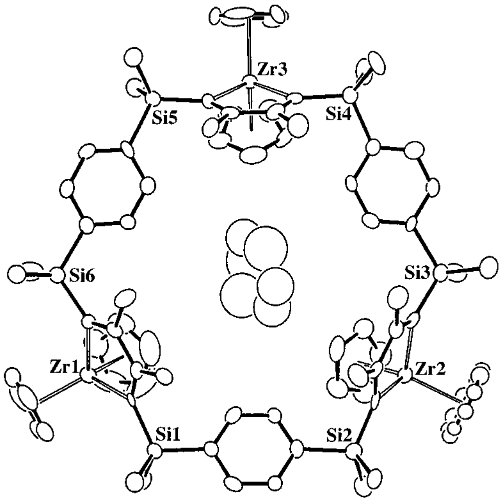

Figure 4. ORTEP diagram of macrocycle **15**. A disordered molecule of benzene is located in the center of the macrocycle.

phenyl groups are all roughly coplanar with the Si atoms of the ring, while the dienyl rings are strongly tilted with respect to this plane. The linkages between the Si atoms are approximately linear, and the cavity size may be described by transannular Si⋯Si distances of 12.87, 13.41, and 13.42 Å.

Colorless needles of **16** were grown from an acetonitrile solution. Selected intramolecular distances and angles are listed in Table 3, and an ORTEP view is shown in Figure 5. In contrast to the nearly planar structure of the parent macrocycle **15**, molecules of **16** adopt a cyclohexane-like chair conformation, which is presumably due to the conversion of cis metallacycle rings to trans-dienyl units. In the solid state, the macrocycles are disordered by a crystallographic inversion center which interchanges transannular phenyl and dienyl groups. These rings are somewhat irregular in shape, as indicated by inequivalent transannular Si−Si distances of 14.22, 11.81, and 12.75 Å, and they are stacked in columns along the *a* direction of the unit cell.

Polymer **6** also undergoes a clean thermal degradation in THF, but in this case a dimeric (rather than a trimeric) macrocycle is formed (Scheme 3). This change in reaction stoichiometry reflects differences in the spacer group geometry. Compound **18** has a very low solubility in hydrocarbon solvents at room temperature and its ^{1}H NMR spectrum, recorded in toluene-d_8 at 110 °C, revealed two sets of signals for both the silylmethyl and cyclopentadienyl groups. The appearance of this spectrum is invariant from −70 to 120 °C, and the two cyclopentadienyl and two silylmethyl resonances do not coalesce up to 120 °C in toluene-d_8.

Table 3. Selected Intramolecular Distances and Angles for **16**

(a) Intramolecular Distances (Å)

Si(1)−C(1)	1.98(3)	C(7)−C(8)	1.38(3)
Si(1′)−C(16)	1.88(3)	C(8)−C(9)	1.54(3)
Si(1′)−C(19)	1.84(3)	C(9)−C(10)	1.27(3)
Si(1)−C(34)	1.85(3)	C(19)−C(20)	1.43(3)
Si(2)−C(4)	2.07(3)	C(20)−C(21)	1.53(3)
Si(2)−C(7)	1.62(2)	C(21)−C(22)	1.38(3)
Si(2′)−C(22)	1.77(2)	C(31)−C(32)	1.40(3)
Si(2′)−C(25)	2.13(3)	C(32)−C(33)	1.50(3)
Si(3)−C(10)	1.92(2)	C(33)−C(34)	1.42(3)
Si(3)−C(13)	2.12(3)	Si(1)−Si(1′)	14.22
Si(3′)−C(28)	1.86(2)	Si(2)−Si(2′)	11.81
Si(3′)−C(31)	1.67(2)	Si(3)−Si(3′)	12.75

(b) Bond Angles (Deg)

C(1)−Si(1)−C(34)	108.4(11)	C(9)−C(10)−Si(3)	126.1(22)
C(4)−Si(2)−C(7)	117.5(9)	Si(1′)−C(19)−C(20)	114.1(20)
C(10)−Si(3)−C(13)	95.0(10)	C(19)−C(20)−C(21)	113.1(21)
C(16)−Si(1′)−C(19)	108.5(11)	C(20)−C(21)−C(22)	117.1(22)
C(22)−Si(2′)−C(25)	95.6(10)	C(21)−C(22)−Si(2′)	121.3(20)
C(28)−Si(3′)−C(31)	126.5(11)	Si(3′)−C(31)−C(32)	125.6(18)
Si(2)−C(7)−C(8)	121.9(16)	C(31)−C(32)−C(33)	119.1(22)
C(7)−C(8)−C(9)	120.0(20)	C(32)−C(33)−C(34)	115.8(24)
C(8)−C(9)−C(10)	121.4(22)	C(33)−C(34)−Si(1)	118.0(21)

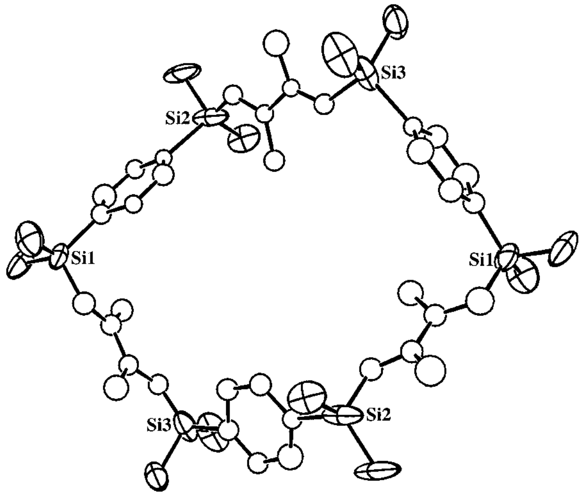

Figure 5. ORTEP diagram of macrocycle **16**.

Hydrolysis of **18** with hydrochloric acid afforded macrocycle **19** in high yield. The ^{1}H and ^{13}C{^{1}H} NMR spectroscopic data for **19** closely correspond to those for macrocycle **16**, and the dimeric structure of macrocycle **19** was confirmed by high-resolution mass spectroscopy.

Air-sensitive, yellow crystals of **18** were obtained by slow cooling of a hot THF solution. Selected intramolecular distances and angles are listed in Table 4, and an ORTEP view of this compound is shown in Figure 6. In this molecule, there is a crystallographic inversion center which relates both the phenylene and the zirconacyclopentadiene rings. The two sets of inequivalent cyclopentadienyl ligands are consistent with the solution-phase structure, as determined by NMR spectroscopy. The molecule contains a planar Si_4 core, with a maximum deviation from the Si_4 least squares plane of 0.05 Å. In addition, the two 1,3-phenylene groups lie in this Si_4 least squares plane, with the dihedral angles between the phenylene and Si_4 least squares planes of only 3.1°. A crystallographic C_2 axis passes through the two phenylene groups. The zirconacyclopentadiene

Scheme 3

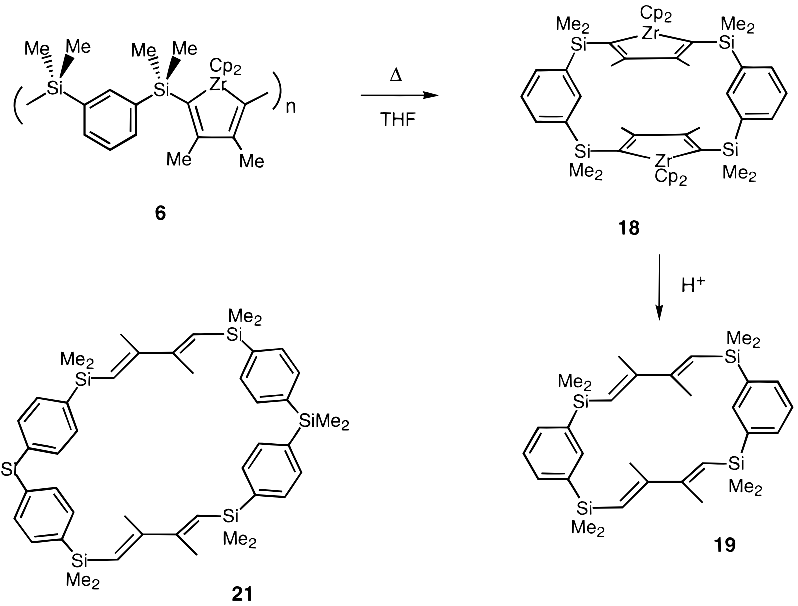

Table 4. Selected Intramolecular Distances and Angles for **18**[a]

(a) Intramolecular Distances (Å)			
Zr(1)−C(8)	2.254(4)	C(11)−C(12)	1.356(5)
Zr(1)−C(12)	2.254(4)	C(12)−Si(2*)	1.869(4)
Si(1)−C(8)	1.860(4)	Zr(1)−Cp(1)	2.230
C(8)−C(10)	1.366(5)	Zr(1)−Cp(2)	2.233
C(10)−C(11)	1.511(5)	Si(1)−Si(1*)	8.910
(b) Bond Angles (deg)			
C(8)−Zr(1)−C(12)	81.1(1)	C(11)−C(12)−Zr(1)	108.0(3)
C(2)−Si(1)−C(8)	114.3(2)	Zr(1)−C(8)−C(10)	108.1(3)
C(8)−C(10)−C(11)	121.0(3)	C(12)−Si(2*)−C(6*)	113.4(2)
C(10)−C(11)−C(12)	121.8(3)	Cp(1)−Zr(1)−Cp(2)	135.8

[a] Atoms with * indicate the crystallographic inversion symmetry.

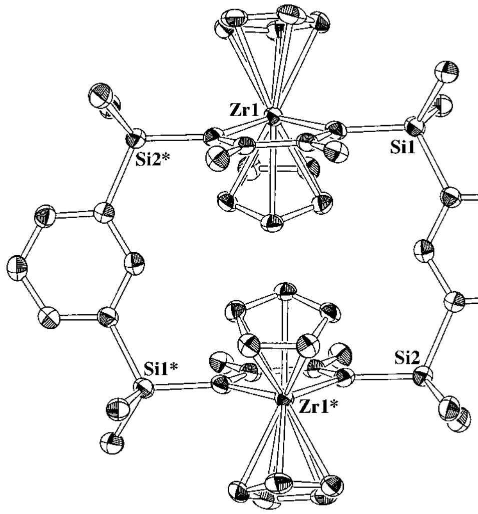

Figure 6. ORTEP diagram of macrocycle **18**.

rings are parallel to each other, with a dihedral angle of only 0.5°. Both of the metallacycles are roughly perpendicular to the Si_4 least squares plane, with a dihedral angle of 84.1°. The two zirconocene fragments lie on opposite sides of the macrocyclic ring, such that the molecule possesses crystallographic inversion symmetry. The cavity size for this macrocycle may be described by the transannular Si···Si distance of 8.9 Å. All bond lengths and angles for the zirconacyclopentadiene fragments appear normal and close to the corresponding values for the zirconacyclopentadiene fragments in macrocycle **15**. These values also correspond well to those for 2,5-bis(trimethylsilyl)-3,4-diphenylzirconacyclopentadiene, which exhibits an average Zr−Cp distance of 2.230 (3), a Zr−C(α) distance of 2.265 (2) Å, and a C(α)−Zr−C(α) angle of 82.6(1)°.[10b] In the solid state, macrocycle **18** contains two sets of inequivalent cyclopentadienyl ligands, which is consistent with the solution structure as determined by ^1H and ^{13}C NMR spectroscopy.

Similarly, the nonlinear diyne **4** was directly coupled to the dimeric zirconocene derivative **20**, by heating the reaction mixture gently to 65 °C for 1 h. Macrocycle **20** was isolated by crystallization from dichloromethane/hexane in 82% yield and completely characterized. This species was then efficiently hydrolyzed to macrocycle **21** (Scheme 3). The molecularity of the latter compound was established by high-resolution mass spectroscopy.

Interestingly, if the spacer group is reduced to a single Si atom ($MeC{\equiv}CSiMe_2C{\equiv}CMe$), the hexameric coupling product **22** (Scheme 4) is isolated in high yield, after heating the reaction mixture (65 °C, 3 h) to affect complete conversion to the macrocycle. This compound is quite insoluble and was obtained from the reaction mixture as an analytically pure, yellow precipitate. Its characterization as a hexamer was inferred from its clean conversion to the hydrolyzed product **23** (Scheme 4), which is soluble in toluene, THF, and dichloromethane. The latter macrocycle was characterized by combustion analysis and by NMR and high-resolution mass spectroscopy. Given the ability of $-CH{=}CMe\text{-}CMe{=}CH-$ to act as a linear spacer group, we propose that **23** has a structure analogous to that for **16**. The tetrahedral angle at silicon should facilitate the formation of a chairlike cyclohexane geometry in this case.

Polymer **7**, like polymer **5**, contains a linear (but longer) spacer group ($4,4'\text{-}Me_2SiC_6H_4C_6H_4SiMe_2$). Thermolysis of a THF solution of polymer **7** under the conditions used to obtain **15** did not cleanly generate the expected trimeric macrocycle **24**. Instead, an equilibrium mixture of **7** and **24** was obtained (Scheme 5). This equilibrium is highly dependent on the concentration of the total solute in the solvent. In dilute solution (0.5 g/70 mL of THF) the equilibrium lies heavily on the side of the macrocycle (as determined by GPC analysis), while in concentrated solution (0.5 g/5 mL of THF) the polymer is the predominant species. Removal of THF from the dilute solution

Scheme 4

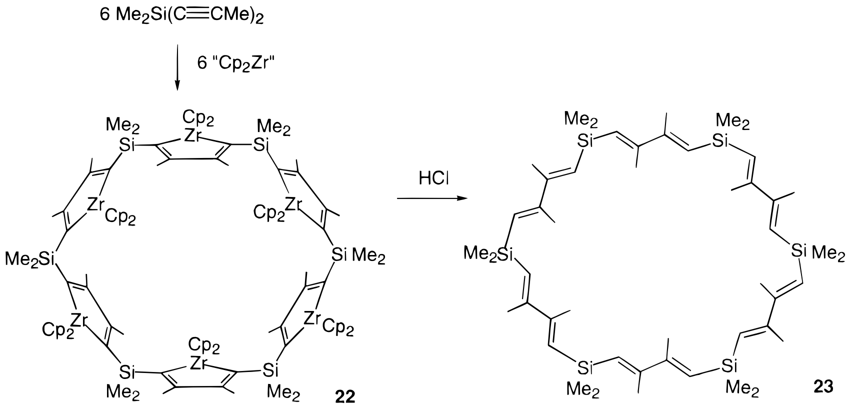

Scheme 5

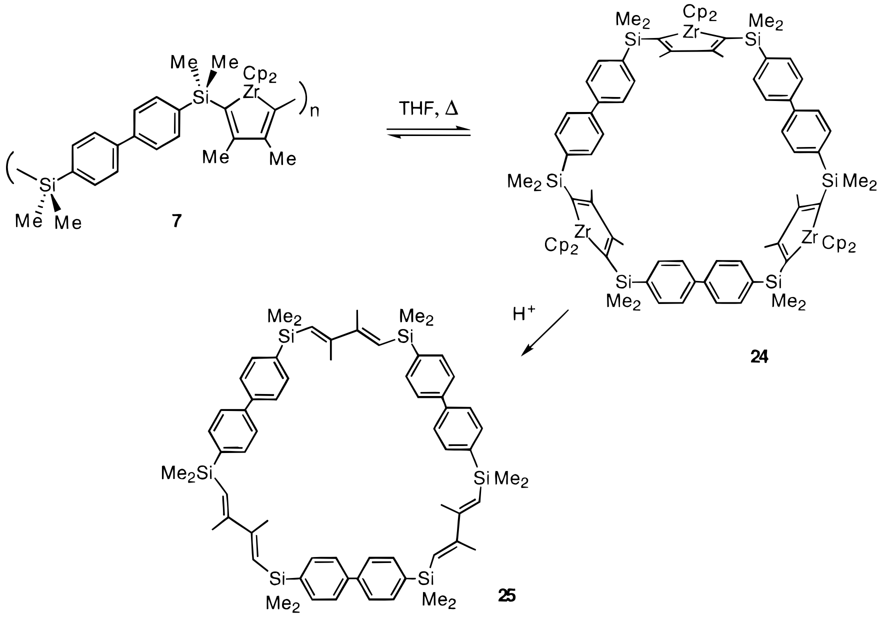

gave a mixture of **7** (ca. 10%, by GPC) and **24** (ca. 90%, by GPC). Attempts to separate the macrocycle from the polymer by recrystallization failed, presumably due to the very similar solubilities of the macrocycle and low molecular weight oligomers.

Macrocycle **24** reacts with hydrochloric acid to form the corresponding cyclophane **25**, which was separated from zirconocene dichloride by extraction with hexane. The trimeric nature of this macrocycle was confirmed by high-resolution mass spectroscopy. The NMR data for macrocycles **24** and **25** closely resemble those for polymer **7** and are consistent with the structures shown in Scheme 5. Unfortunately, we have not been able to obtain crystals of **24** or **25** that are suitable for X-ray diffraction studies. However, the cavity sizes for these macrocycles were calculated to be approximately 17 and 18 Å, respectively.[17]

The electronic properties of these polymers have been studied by UV−vis spectroscopy, and the $\lambda_{\max}$ values are listed in Table 5. Due to their σ/π conjugated nature, these polymers all have high band gaps, as indicated by their low $\lambda_{\max}$ values. The $\lambda_{\max}$ value for **5** (226 nm) is at somewhat lower energy than that for the model compound **8** (214 nm), suggesting only slight conjugation between the monomer units in **5**, as would be expected for cis-diene units and a σ/π system of this type.[18] Polymer **6**, with the 1,3-phenylene linker, has a lower $\lambda_{\max}$ value (214 nm) than the polymer with the 1,4-phenylene linker (**5**, 226 nm), indicating that the *para* phenylene group is slightly more effective at delocalizing electron density. The $\lambda_{\max}$ value for polymer **11** (262 nm) reflects the greater delocalization for the trans-dienyl units (vs the cis-dienyl units in **5**).[19] The similar $\lambda_{\max}$ values for polymer **11** and the model compound **9** (260 nm) suggest that there is little or no conjugation between

Table 5. λ_{Max} Values (nm) for the σ/π Conjugated Polymers and Model Compounds[a]

metallacycles	**8**	**5**	**6**	**7**	**15**	**18**	**24**
absorption bands	214	226	214	266	226	214	264
hydrolyzed species	**9**	**11**	**12**	**13**	**16**	**19**	**25**
absorption bands	260	262	260	268	256	260	266

[a] THF solvent.

---

[17] The cavity sizes of macrocycles **19** and **20** were estimated based on the crystal structures of macrocycles **14** and **15**. The structures of macrocycles **14** and **15** were manipulated with the Chem 3D graphic program, by replacing the phenylene spacers in **14** and **15** with a biphenylene spacer. The maximum Si···Si distances in **19** and **20** were then estimated as 17 and 18 Å, respectively.

[18] (a) Fang, M.; Watanabe, A.; Matsuda, M. *J. Organomet. Chem.* **1995**, *489*, 15. (b) Fang, M.; Watanabe, A.; Matsuda, M. *Chem. Lett.* **1994**, 13. (c) Corriu, R. J. P.; Douglas, W. E.; Yang, Z. X. *J. Organomet. Chem.* **1991**, *417*, C50. (d) Chicart, P.; Corriu, R. J. P.; Moreau, J. J. E. *Chem. Mater.* **1991**, *3*, 8.

[19] Hendrickson, J. B.; Cram, D. J.; Hammond, G. S. *Organic Chemistry;* McGraw-Hill: New York, 1970; Chapter 7, pp 246−256.

monomer units. In polymers with only a monosilylene spacer, the $SiMe_2$ group acts primarily as an insulator to interrupt electron delocalization along the polymer chain.[18] This lack of electron delocalization has also been observed in the related polymer $(-SiMe_2C_6H_4-)_n$, whose λ_{max} value of 236 nm is mainly due to the phenylene chromophore.[18a]

Macrocycles **15**, **18,** and **24** have λ_{max} values that are similar to those for the corresponding polymers **5**, **6,** and **7**. Interestingly, the hydrolyzed trimer **16** exhibits a λ_{max} value of 254 nm, which is slightly lower than that of the hydrolyzed polymer **11**, presumably because the trans-diene units in the polymer chain are less constrained and thus more delocalized than in the trimeric macrocycle.

Discussion

The zirconocene-coupling of silicon-substituted diynes is highly regiospecific and affords organosilicon polymers with zirconacyclopentadiene repeat units in the main chain. These metal-containing polymers provide starting points for the synthesis of organosilicon, or derivatized organosilicon, polymers. More interestingly, they undergo facile and clean degradations at fairly low temperatures to metal-containing macrocycles. Thus, this chemistry represents a simple and efficient method for the relatively large scale synthesis of macrocyclic compounds. This is noteworthy, since syntheses for macrocycles often require dilute conditions and tedious separations, and give low yields.[20] Note that there has been considerable recent interest in metal-containing macrocycles as catalysts, sensors, and precursors to novel cyclophane structures.[21]

Diynes **1** and **3** with parallel alkynyl groups have been observed to undergo zirconocene-coupling to trimeric macrocyles. The nonlinear $1,3-Me_2SiC_6H_4SiMe_2$ and $Me_2SiC_6H_4SiMe_2C_6H_4SiMe_2$ spacer groups, however, result in formation of a dimeric macrocycle. With the very small $SiMe_2$ spacer group, a hexameric product is obtained. Thus, di-, tri-, and hexafunctional rings may be constructed starting with the appropriate spacer group geometry. Whereas formation of $[1,4-Me_2SiC_6H_4SiMe_2C_4Me_2ZrCp_2]_3$ (**15**) from the polymer is essentially quantitative under various conditions, the analogous synthesis of $[4,4'-Me_2SiC_6H_4C_6H_4SiMe_2C_4Me_2ZrCp_2]_3$ (**24**) requires dilute conditions. Therefore the zirconocene-coupling method for forming macrocycles with $-SiMe_2ArSiMe_2-$ spacer groups appears to be somewhat restricted with respect to accessible cavity sizes. In related work, we have found that diynes with terminal silyl substituents have a greater tendency to form macrocyclic (vs polymeric) structures,[2b] and we are currently exploring the synthesis of very large macrocycles from such monomers.[22]

The metal-containing polymers (and presumably macrocycles) reported here are labile and readily open via the reversible cleavage of C$-$C bonds in the zirconacyclopentadiene units. In this way, facile interconversions of macrocyclic and oligomeric structures allow for the most thermodynamically favored structure to predominate. This reactivity may be attributed to the reversibility of diyne coupling, which is promoted by silicon substituents in the diyne. A similar process was characterized by Erker et al., who proposed that the zirconacyclopentadiene complex $Cp_2ZrC_4(SiMe_3)_2Ph_2$ is in equilibrium with the bis(alkyne) complex $Cp_2Zr(\eta^2-Me_3SiC{\equiv}CPh)_2$, based on its reaction with PMe_3 to give $Cp_2Zr(\eta^2-Me_3SiC{\equiv}CPh)(PMe_3)$ and $Me_3SiC{\equiv}CPh$.[10a] Similarly, the zirconacyclopentadiene groups in the polymer backbones of **5**$-$**7** may undergo reversible cleavages of the type shown in eq 2. This facile reversibility appears to provide a low-energy pathway to the thermodynamic product, which is the smallest strain-free ring which can form. In THF solution, this process is probably assisted by the formation of adducts such as **A**, which stabilize intermediates in the chain-scission process. Recently an adduct closely related to **A**, $Cp_2Zr(\eta^2-Me_3SiC{\equiv}CSiMe_3)(THF)$, was isolated and structurally characterized.[23] Consistent with this, we observe that the polymer-to-macrocycle conversions proceed more rapidly and more cleanly in THF (vs benzene). Note that after the "metallacycle chemistry" acts to assemble the diyne-zirconocene systems into pure samples of macrocycles, these labile ring systems are readily converted to very nonlabile carbosilane rings after hydrolysis.

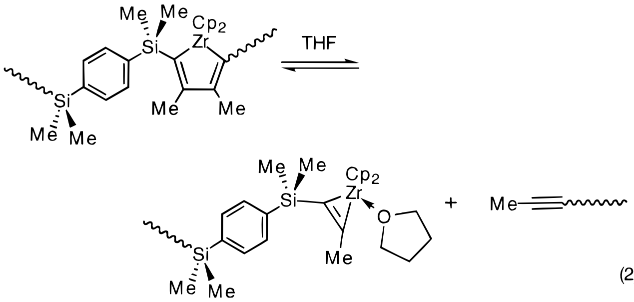

(2)

A

Whereas the macrocycles with 1,3- and 1,4-phenylene spacer groups are formed in very high yield, the longer 4,4′-biphenylene group results in a macrocycle that is in equilibrium with its polymeric form. Polymer ring-chain interconversion is a well-known phenomenon for both organic and inorganic polymers.[15,24] For example, in the dimethylsiloxane system, the cyclic trimer $(OSiMe_2)_3$ and the tetramer $(OSiMe_2)_4$ polymerize readily with anionic or cationic initiators to yield poly(dimethylsiloxane), $(OSiMe_2)_n$, which depolymerizes at tem-

---

[20] (a) Vögtle, F. *Cyclophane Chemistry*; John Wiley & Sons: Chichester, West Sussex, 1993. (b) Dietrich, B.; Viout, P.; Lehn, J.-M. *Macrocyclic Chemistry: Aspects of Organic and Inorganic Supramolecular Chemistry;* VCH: Weinheim, New York, 1993. (c) Vögtle, F. *Supramolecular Chemistry*; John Wiley & Sons: Chichester, West Sussex, 1991.

[21] Representative publications include: (a) Plenio, H. *Angew. Chem., Int. Ed. Engl.* **1997**, *36*, 348. (b) Olenyuk, B.; Whiteford, J. A.; Stang, P. J. *J. Am. Chem. Soc.* **1996**, *118*, 8221. (c) Stang, P. J.; Cao, D. H.; Saito, S.; Arif, A. M. *J. Am. Chem. Soc.* **1995**, *117*, 6273. (d) Bradshaw, J. D.; Guo, L.; Tessier, C. A.; Youngs, W. J. *Organometallics* **1996**, *15*, 2582. (e) Irwin, M. J.; Rendina, L. M.; Vittal, J. J.; Puddephatt, R. J. *J. Chem. Soc., Chem. Commun.* **1996**, 1281. (f) Barlow, S.; O'Hare, D. *Organometallics* **1996**, *15*, 3885. (g) Rubin, Y.; Knobler, C. B.; Diederich, F. *J. Am. Chem. Soc.* **1990**, *112*, 4966. (h) Beer, P. D. *Adv. Mater.* **1994**, *6*, 607. (i) Slone, R. V.; Hupp, J. T.; Stern, C. L.; Albrechtschmitt, T. E. *Inorg. Chem.* **1996**, *35*, 4096. (j) Altmann, M.; Friedrich, J.; Beer, F.; Reuter, R.; Enkelmann, V.; Bunz, U. H. F. *J. Am. Chem. Soc.* **1997**, *119*, 1472. (k) Grossman, B.; Heinze, J.; Herdtweck, E.; Köhler, F. H.; Nöth, H.; Schwenk, H.; Spiegler, M.; Wachter, W.; Weber, B. *Angew. Chem., Int. Ed. Engl.* **1997**, *36*, 387. (l) Jacopozzi, P.; Dalcanale, E. *Angew. Chem., Int. Ed. Engl.* **1997**, *36*, 613. (m) Haley, M. M.; Langsdorf, B. L. *J. Chem. Soc., Chem. Commun.* **1997**, 1121. (n) Kickham, J. E.; Loeb, S. J. *J. Chem. Soc., Chem. Commun.* **1993**, 18481. (o) Walter, C. J.; Sanders, J. K. M. *Angew. Chem., Int. Ed. Engl.* **1995**, *34*, 217. (p) Coolen, H. K. A. C.; Meeuwis, J. A. M.; van Leeuwen, P. W. N. M.; Nolte, R. J. M. *J. Am. Chem. Soc.* **1995**, *117*, 11906.

[22] Harder, G.; Tilley, T. D., work in progress.

[23] Rosenthal, U.; Ohff, A.; Michalik, M.; Gorls, H.; Burlakov, V. V.; Shur, V. B. *Angew. Chem., Int. Ed. Engl.* **1993**, *32*, 1193.

[24] (a) Gee, G. *Chem. Soc. (London), Spec. Publ.* **1961**, *15*, 67. (b) Tobolsky, A. V. *J. Polymer Sci.* **1957**, *25*, 220. (c) Tobolsky, A. V. *J. Polymer Sci.* **1958**, *31*, 126. (d) Tobolsky, A. V.; Eisenberg, A. *J. Am. Chem. Soc.* **1959**, *81*, 780. (e) Tobolsky, A. V.; Eisenberg, A. *J. Am. Chem. Soc.* **1959**, *81*, 2303. (f) Tobolsky, A. V.; Eisenberg, A. *J. Am. Chem. Soc.* **1960**, *82*, 289. (g) Tobolsky, A. V.; MacKnight, W. J. in *Polymeric Sulfur and Related Polymers;* Mark, H. F., Immergut, E. H., Eds.; Wiley-Interscience: New York; 1965.

peratures above 300 °C to yield mainly the cyclic tetramer. Rhombic sulfur, S_8, can be polymerized at temperatures above 160 °C to polymeric sulfur S_n, which depolymerizes back to cyclic S_8 at higher temperature. In the absence of ring strain and significant differences between torsional and vibrational entropies for the polymer and macrocycle, the polymer-to-macrocycles conversion is expected to be thermodynamically favored at most temperatures due to the greater translational entropy for a collection of n rings (nR) vs a linear polymer chain (R_n). As the size of the ring in a ring-polymer equilibrium increases, the entropy difference between rings and polymers for a given number of monomer units decreases. With larger macrocycles, then, there is less of a thermodynamic bias in favor of the macrocyclic product.

To our knowledge, the near-quantitative formation of metal-containing macrocycles by the degradation of polymers is without precedent. In a few other cases, polymer degradation or ring enlargement oligomerization has been applied to the synthesis of macrocycles.[20b,25,26] By these means macrocycles with a distribution of sizes are typically formed, and tedious separations are usually unavoidable. For example, Ito recently reported the synthesis of a mixture of organosilicon macrocycles via palladium-catalyzed ring-enlargement oligomerization of the cyclic disilane 1,1,2,2-tetramethyl-1,2-disilacyclopentane to a mixture of cyclic oligomers consisting of dimer (3%), trimer (32%), tetramer (34%), pentamer (14%), hexamer (6%), and heptamer (3%).[25]

We anticipate that macrocyclization reactions of the type described here will be of use in the synthesis of new ring structures with a variety of functions. This synthetic method is simple and versatile, particularly since macrocycles with different sizes and shapes are available via manipulation of the diyne structure. Future investigations will focus on the use of this method for construction of large rings, cages, and functionalized macrocycles.

Experimental Section

All manipulations were performed under an inert atmosphere of nitrogen using either standard Schlenk techniques or a Vacuum Atmospheres glovebox. Dry, oxygen-free solvents were employed throughout. All solvents were distilled from sodium/benzophenone ketyl. Benzene-d_6 was purified by vacuum distillation from Na/K alloy. Elemental analyses were performed by the UCB Microanalytical Laboratory or Desert Analytics. IR spectra were recorded on a Mattson Galaxy Series 3000 spectrometer. UV−vis spectra were obtained with a HP 8452A spectrophotometer. NMR spectra were recorded on a Bruker AMX (300 MHz), a Varian Bruker AMX (400 MHz), or a Bruker DRX (500 MHz) spectrometer. The molecular weights of the polymers were determined by gel permeation chromatography (GPC; Waters R401 Differential Refractometer Detector; Waters 501 HPLC Pump) with THF as the eluting solvent and polystyrene standards. Thermal analyses were performed on a DuPont 951 Thermogravimetric Analyzer attached to a 910 DSC cell base. Ramp rates were 10 °C/min for TGA analyses and 2 °C/min for DSC analyses. Zirconocene dichloride (Strem) and n-butyllithium solution (Aldrich) were used as received. The compounds 1,4-$ClMe_2SiC_6H_4SiMe_2Cl$, 1,3-$ClMe_2SiC_6H_4SiMe_2Cl$ and 4,4′-$ClMe_2SiC_6H_4C_6H_4SiMe_2Cl$ were prepared from 1,4-$(EtO)Me_2SiC_6H_4SiMe_2(OEt)$, 1,3-$(EtO)Me_2SiC_6H_4SiMe_2(OEt)$, and 4,4′-$(EtO)Me_2SiC_6H_4C_6H_4SiMe_2(OEt)$, respectively, via a modified literature procedure.[11] The compounds $BrC_6H_4SiMe_2Cl$[27] and $Me_2Si(C{\equiv}CMe)_2$[28] were also prepared by literature procedures.

1,4-$(EtO)Me_2SiC_6H_4SiMe_2(OEt)$. A three-neck 1000-mL round-bottom flask equipped with a reflux condenser and an addition funnel was charged with $Me_2Si(OEt)_2$ (144 mL, 125 g, 840 mmol), Mg (22.0 g, 900 mmol), and THF (200 mL). A THF solution (200 mL) of 1,4-BrC_6H_4Br (97.0 g, 410 mmol) was added dropwise to the flask. After the first few drops were added, the flask was warmed gently with a hot water bath to initiate the reaction. After the reaction was initiated, the solution temperature was maintained at 30 °C by controlling the rate of addition, which took approximately 4 h. The reaction mixture was then refluxed for 8 h, and then the solvent was removed in vacuo. Hexane (300 mL) was added to the reaction flask, and the mixture was filtered. The resulting solid was extracted with more hexane (2 × 50 mL), and the extracts were combined. The volatile material was removed in vacuo, and the residue was distilled to afford 73 g (63%) of colorless liquid, bp 85−88 °C (0.02 Torr). ^1H NMR (benzene-d_6, 300 MHz): δ 7.66 (s, 4 H, C_6H_4), 3.56 (q, 4 H, $J = 6.9$, OCH_2CH_3), 1.10 (t, 6 H, $J_{HH} = 6.9$ Hz, OCH_2CH_3), 0.34 (s, 12 H, $SiMe_2$). $^{13}C\{^1H\}$ NMR (benzene-d_6, 100.6 MHz): δ 139.81 (C_6H_4, C), 133.87 (C_6H_4, CH), 58.57 (OCH_2CH_3), 18.62 (OCH_2CH_3), −1.64 ($SiMe_2$). The compound was pure by both ^1H and $^{13}C\{^1H\}$ NMR spectroscopy.

1,4-$ClMe_2SiC_6H_4SiMe_2Cl$. A 100-mL thick-walled flask equipped with a Kontes valve was charged with 1,4-$(EtO)Me_2SiC_6H_4SiMe_2(OEt)$ (12.0 g, 42.0 mmol) and acetyl chloride (14.0 g, 180 mmol). The flask was degassed, sealed, and heated to 80 °C for 6 h. The volatile materials were removed in vacuo to give 10.9 g (98%) of product as white crystals. ^1H NMR (benzene-d_6, 400 MHz): δ 7.50 (s, 4 H, C_6H_4), 0.42 (s, 12 H, $SiMe_2$). $^{13}C\{^1H\}$ NMR (benzene-d_6, 100.6 MHz): δ 139.51 (C_6H_4, C), 134.12 (C_6H_4, CH), −1.51 ($SiMe_2$). mp 65−67 °C. The compound was pure by both ^1H and $^{13}C\{^1H\}$ NMR spectroscopy.

1,3-$(EtO)Me_2SiC_6H_4SiMe_2(OEt)$. This compound was prepared from $Me_2Si(OEt)_2$, Mg, and 1,3-BrC_6H_4Br as a colorless liquid in 57% yield, by the procedure for 1,4-$(EtO)Me_2SiC_6H_4SiMe_2(OEt)$, bp 77−78 °C (0.02 Torr). ^1H NMR (benzene-d_6, 400 MHz): δ 8.07 (s, 1 H, C_6H_4), 8.63 (d, $J_{HH} = 7.6$ Hz, 2 H, C_6H_4), 7.30 (t, $J_{HH} = 7.6$ Hz, 2 H, C_6H_4), 3.57 (q, 4 H, $J_{HH} = 7.2$ Hz, OCH_2CH_3), 1.10 (t, 6 H, $J_{HH} = 7.2$ Hz, OCH_2CH_3), 0.34 (s, 12 H, $SiMe_2$). $^{13}C\{^1H\}$ NMR (benzene-d_6, 100.6 MHz): δ 138.82 (C_6H_4, CH), 137.83 (C_6H_4, CH), 135.01 (C_6H_4, CH), 127.60 (C_6H_4, C), 58.64 (OCH_2CH_3), 18.70 (OCH_2CH_3), −1.47 ($SiMe_2$).

1,3-$ClMe_2SiC_6H_4SiMe_2Cl$. This compound was prepared from 1,3-$ClMe_2SiC_6H_4SiMe_2Cl$ and acetyl chloride in 97% yield, by the procedure used for 1,4-$(EtO)Me_2SiC_6H_4SiMe_2(OEt)$. ^1H NMR (benzene-d_6, 400 MHz): δ 7.99 (s, 1 H, C_6H_4), 7.54 (d, $J_{HH} = 7.6$ Hz, 2 H, C_6H_4), 7.18 (t, $J_{HH} = 7.6$ Hz, 1 H, C_6H_4), 0.44 (s, 12 H, $SiMe_2$). $^{13}C\{^1H\}$ NMR (benzene-d_6, 100.6 MHz): δ 137.75 (C_6H_4, CH), 136.32 (C_6H_4, CH), 135.33 (C_6H_4, CH), 128.02 (C_6H_4, C), 1.94 ($SiMe_2$).

4,4′-$(EtO)Me_2SiC_6H_4C_6H_4SiMe_2(OEt)$. This compound was prepared from $Me_2Si(OEt)_2$, Mg, and 4,4′-$BrC_6H_4C_6H_4Br$ as a colorless liquid in 57% yield, by the procedure used for 1,4-$(EtO)Me_2SiC_6H_4SiMe_2(OEt)$ bp 153−154 °C/0.02 Torr. ^1H NMR (benzene-d_6, 400 MHz): δ 7.66 (d, 4 H, $J_{HH} = 8.4$ Hz, C_6H_4), 7.59 (d, 4 H, $J_{HH} = 8.4$ Hz, C_6H_4), 3.59 (q, 4 H, $J_{HH} = 6.9$ Hz, OCH_2CH_3), 1.13 (t, 6 H, $J_{HH} = 6.9$ Hz, OCH_2CH_3), 0.37 (s, 12 H, $SiMe_2$). $^{13}C\{^1H\}$ NMR (benzene-d_6, 100.6 MHz): δ 142.66 (C_6H_4, C), 137.51 (C_6H_4, C), 134.45 (C_6H_4, CH), 126.85 (C_6H_4, CH), 58.68 (OCH_2CH_3), 18.73 (OCH_2CH_3), −1.47 ($SiMe_2$).

4,4′-$ClMe_2SiC_6H_4C_6H_4SiMe_2Cl$. This compound was prepared from 4,4-$(EtO)Me_2SiC_6H_4C_6H_4SiMe_2(OEt)$ and acetyl chloride in 95% yield, by the procedure used for 1,4-$(EtO)Me_2SiC_6H_4SiMe_2(OEt)$. ^1H NMR (benzene-d_6, 400 MHz): δ 7.58 (d, $J_{HH} = 8.4$ Hz, 4 H, C_6H_4), 7.48 (s, $J_{HH} = 8.4$ Hz, 4 H, C_6H_4), 0.50 (s, 12 H, $SiMe_2$). $^{13}C\{^1H\}$ NMR (benzene-d_6, 100.6 MHz): δ 142.90 (C_6H_4, C), 135.60 (C_6H_4, C), 134.08 (C_6H_4, CH), 127.13 (C_6H_4, CH), 2.04 ($SiMe_2$).

$BrC_6H_4SiMe_2(C{\equiv}CMe)$. This compound was prepared as a colorless liquid in 85% yield after distillation at 75 °C/0.1 Torr from reaction of $BrC_6H_4SiMe_2Cl$ with $CH_3C{\equiv}CLi$, via a procedure similar to that

---

[25] (a) Suginome, M.; Oike, H.; Ito, Y. *J. Am. Chem. Soc.* **1995**, *117*, 1665−1666. (b) Suginome, M.; Oike, H.; Shuff, P. H.; Ito, Y. *Organometallics* **1996**, *15*, 2170−2178.

[26] Brady, P. A.; Bonar-Law, R. P.; Rowan, S. J.; Suckling, C. J.; Sanders, J. K. M. *J. Chem. Soc., Chem. Commun.* **1996**, 319.

[27] van Walree, C. A.; Roest, M. R.; Schuddeboom, W.; Jenneskens, L. W.; Verhoeven, J. W.; Warman, J. M.; Kooijman, H.; Spek, A. L. *J. Am. Chem. Soc.* **1996**, *118*, 8395.

[28] Köster, R.; Seidel, G.; Süss, J.; Wrackmeyer, B. *Chem. Ber.* **1993**, *126*, 1107.

used for **1**. ^{1}H NMR ($CDCl_3$, 400 Hz): δ 7.51 (s, 4 H, C_6H_4), 1.95 (s, 3 H, C≡C*Me*), 0.41 (s, 6 H, SiMe_2). $^{13}C\{^1H\}$ NMR ($CDCl_3$, 100.6 Hz): δ 136.35 (C_6H_4, C), 135.26, 130.96 (C_6H_4, CH), 124.15 (C_6H_4, C), 105.31, 81.25 (*C*≡*C*), 4.99 (C≡C*Me*), −1.03 (SiMe_2). Anal. Calcd for $C_{11}H_{13}BrSi$: C, 52.18; H, 5.17. Found: C, 52.35; H, 5.36.

1,4-MeC≡C(Me_2Si)C_6H_4(SiMe_2)C≡CMe (1). Propyne (1.50 g, 37.5 mmol) was condensed at −78 °C into a 250-mL round-bottom flask containing 100 mL of THF. *n*-Butyllithium (1.60 M, 23.4 mL, 37.5 mmol) was then added dropwise at −78 °C. After the reaction mixture was warmed to room temperature, a white precipitate formed. The flask was stirred at room temperature for 30 min, and then a THF solution (15 mL) of 1,4-$ClMe_2SiC_6H_4SiMe_2Cl$ (5.00 g, 19.0 mmol) was added. The precipitate dissolved gradually, yielding a clear solution. All the volatile materials were removed in vacuo, and the product was sublimed to give 4.50 g (88%) of the product as white crystals. ^{1}H NMR (benzene-d_6, 300 MHz): δ 7.76 (s, 4 H, C_6H_4), 1.52 (s, 6 H, CH_3), 0.42 (s, 12 H, SiMe_2). $^{13}C\{^1H\}$ NMR (benzene-d_6, 100.6 MHz): δ 138.96 (C_6H_4, C), 133.50 (C_6H_4, CH), 105.13 (*C*+CSi), 82.13 (C+*C*Si), 4.60 (CH_3), −0.60 (SiMe_2). UV−vis (THF, nm): 270, 276, 294 (shoulder). mp 43.5−45 °C. Anal. Calcd for $C_{16}H_{22}Si_2$: C, 71.04; H, 8.20. Found: C, 70.28; H, 8.34. IR (Nujol): 2179 cm^{-1} (C≡C stretch).

1,3-MeC≡C(Me_2Si)C_6H_4(SiMe_2)C≡CMe (2). Compound **2** was prepared as a colorless liquid in 88% yield from reaction of 1,3-$ClMe_2SiC_6H_4SiMe_2Cl$ with CH_3C≡CLi, via a procedure similar to that used for **1**. ^{1}H NMR (benzene-d_6, 400 MHz): δ 8.25 (s, 1 H, C_6H_4), 7.74 (d, *J* = 7.6, 2 H, C_6H_4), 7.30 (t, *J* = 7.6, 1 H, C_6H_4), 1.52 (s, 6 H, CH_3), 0.43 (s, 12 H, SiMe_2). $^{13}C\{^1H\}$ NMR (benzene-d_6, 100.6 MHz): δ 139.28 (C_6H_4, CH), 137.12 (C_6H_4, CH), 135.16 (C_6H_4, CH), 127.67 (C_6H_4, C), 105.15 (*C*≡CSi), 82.28 (C≡*C*Si), 4.58 (CH_3), −0.50 (SiMe_2). EIMS showed M$^+$ = 270. HRMS calcd for $C_{16}H_{22}Si_2$, 270.126008; found, 270.126476. IR (Nujol): 2183 cm^{-1} (C≡C stretch).

4,4′-MeC≡C(Me_2Si)$C_6H_4C_6H_4$(SiMe_2)C≡CMe (3). Compound **3** was prepared as a white solid in 90% yield from reaction of 4,4′-$ClMe_2SiC_6H_4C_6H_4SiMe_2Cl$ and CH_3C≡CLi, via a procedure similar to that for **1**. Further crystallization from methanol gave **3** as white needles (88%). ^{1}H NMR (benzene-d_6, 400 MHz): δ 7.78 (d, J_{HH} = 8.4 Hz, 4 H, C_6H_4), 7.59 (d, J_{HH} = 8.4 Hz, 4 H, C_6H_4), 1.54 (s, 6 H, CH_3), 0.46 (s, 12 H, SiMe_2). $^{13}C\{^1H\}$ NMR (benzene-d_6, 100.6 MHz): δ 142.54 (C_6H_4, C), 136.72 (C_6H_4, C), 134.71 (C_6H_4, CH), 127.03 (C_6H_4, CH), 105.22 (*C*≡CSi), 82.21 (C≡*C*Si), 4.62 (CH_3), −0.45 (SiMe_2). EIMS showed M$^+$ = 346. HRMS Calcd for $C_{22}H_{26}Si_2$, 346.157308; found, 346.157834. IR (Nujol): 2179 cm^{-1} (C≡C stretch).

$Me_2Si[C_6H_4SiMe_2$(C≡CMe)]$_2$ (4). A 250 mL round-bottom flask was charged with $BrC_6H_4SiMe_2$(C≡CMe) (6.00 g, 23.7 mmol) and a mixture of THF/ether (1:1, 120 mL). The flask was cooled to −78 °C and then *n*-butyllithium (1.6 M/hexane, 14.8 mL, 23.7 mmol) was added dropwise. The mixture was stirred for 30 min at −78 °C. Me_2SiCl_2 (1.43 mL, 11.9 mmol) was then added dropwise, and the temperature of the flask was raised to room temperature over 6 h. The volatile materials were removed in vacuo, and the residue was extracted with dichloromethane (120 mL). The solution was concentrated to 20 mL and then passed through a silica gel (15 × 4.2 cm) column using a mixture of dichlomethane/hexane (1:7) as eluting solvent. The product was obtained as a liquid in 82% yield (3.92 g) after removal of solvent. It was pure by NMR spectroscopy. ^{1}H NMR ($CDCl_3$, 400 Hz): δ 7.66 (d, *J* = 7.8 Hz, 2 H, C_6H_4), 7.58 (d, *J* = 7.8 Hz, 2 H, C_6H_4), 1.96 (s, 3 H, C≡C*Me*), 0.60 (s, 3 H, SiMe_2), 0.44 (s, 6 H, C≡CSiMe_2). $^{13}C\{^1H\}$ NMR ($CDCl_3$, 100.6 Hz): δ 139.22, 138.38 (C_6H_4, C), 133.51, 132.95 (C_6H_4, CH), 104.84, 81.73 (*C*≡*C*), 4.99 (C≡C*Me*), −0.83 (C≡CSiMe_2), −2.58 (SiMe_2). Anal. Calcd for $C_{24}H_{32}Si_3$: C, 71.22; H, 7.97. Found: C, 70.65; H, 7.82.

[(1,4-$Me_2SiC_6H_4SiMe_2)C_4Me_2ZrCp_2]_n$ (5). A 100 mL round-bottom flask was charged with Cp_2ZrCl_2 (4.38 g, 14.9 mmol), **1** (3.90 g, 14.4 mmol), and THF (25 mL). The flask was cooled to −78 °C, and then 1.60 M *n*-butyllithium (18.7 mL, 29.9 mmol) was added dropwise. The flask was allowed to warm to room temperature, and stirring was continued for 48 h. All the volatile materials were removed in vacuo, the residue was extracted into benzene (50 mL), and the resulting solution was filtered through Celite. The clear benzene solution was poured into 200 mL of pentane, resulting in precipitation of the polymer as a yellow powder (6.21 g; 89%). ^{1}H NMR (benzene-d_6, 300 MHz): δ 7.87 (s, 4 H, C_6H_4), 6.10 (s, 10 H, C_5H_5), 1.79 (s, 6 H, C_4Me_2), 0.35 (s, 12 H, SiMe_2). $^{13}C\{^1H\}$ NMR (benzene-d_6, 100.6 MHz): δ 199.15 (ZrC_4Me_2), 149.52 (ZrC_4Me_2), 142.78 (C_6H_4, C), 133.82 (C_6H_4, CH), 111.50 (C_5H_5), 27.55 (ZrC_4Me_2), 2.16 (SiMe_2). M_n = 4600, M_w = 13 000. UV−vis (THF, nm): 214, 226, 328. Anal. Calcd for $C_{26}H_{32}Si_2Zr$: C, 63.48; H, 6.56. Found: C, 62.71; H, 6.56.

[(1,3-$Me_2SiC_6H_4SiMe_2)C_4Me_2ZrCp_2]_n$ (6). The method for polymer **5** was used, starting with Cp_2ZrCl_2 (4.68 g, 16.0 mmol), **2** (4.32 g, 16.0 mmol), and THF (25 mL). The polymer was isolated as a yellow powder (3.9 g; 50%). ^{1}H NMR (benzene-d_6, 400 MHz): δ 8.28 (s, 1 H, C_6H_4), 7.78 (d, J_{HH} = 6.4 Hz, 2 H, C_6H_4), 7.46 (t, J_{HH} = 6.4 Hz, 1 H, C_6H_4), 6.18 (s, 10 H, C_5H_5), 1.84 (s, 6 H, C_4Me_2), 0.39 (s, 12 H, SiMe_2). $^{13}C\{^1H\}$ NMR (benzene-d_6, 100.6 MHz): δ 199.46 (ZrC_4Me_2), 149.47 (ZrC_4Me_2), 141.70 (C_6H_4, CH), 140.00 (C_6H_4, CH), 134.35 (C_6H_4, CH), 127.67 (C_6H_4, C), 111.59 (C_5H_5), 27.61 (ZrC_4Me_2), 2.44 (SiMe_2). M_n = 2600, M_w = 5800. Anal. Calcd for $C_{26}H_{32}Si_2Zr$: C, 63.48; H, 6.56. Found: C, 62.57; H, 6.64.

[(4,4′-$Me_2SiC_6H_4C_6H_4SiMe_2)C_4Me_2ZrCp_2]_n$ (7). The method for polymer **5** was used, starting with Cp_2ZrCl_2 (2.34 g, 8.00 mmol), **3** (2.72 g, 7.85 mmol), and THF (25 mL). The polymer was isolated as a yellow powder (3.45 g; 76%). ^{1}H NMR (benzene-d_6, 400 MHz): δ 7.85 (d, J_{HH} = 8.0 Hz, 4 H, C_6H_4), 7.75 (d, J_{HH} = 8.0 Hz, 4 H, C_6H_4), 6.12 (s, 10 H, C_5H_5), 1.82 (s, 6 H, C_4Me_2), 0.35 (s, 12 H, SiMe_2). $^{13}C\{^1H\}$ NMR (benzene-d_6, 100.6 MHz): δ 199.21 (ZrC_4Me_2), 149.52 (ZrC_4Me_2), 141.62 (C_6H_4, C), 137.80 (C_6H_4, C), 134.93 (C_6H_4, CH), 126.99 (C_6H_4, CH), 111.54 (C_5H_5), 27.55 (ZrC_4Me_2), 2.15 (SiMe_2). M_n = 8500, M_w = 18 000. Anal. Calcd for $C_{32}H_{36}Si_2Zr$: C, 67.66; H, 6.39. Found: C, 66.99; H, 6.45.

$Cp_2ZrC_4(SiMe_2Ph)_2Me_2$ (8). Propyne (1.21 g, 29.9 mmol) was condensed at −78 °C into a 250 mL round-bottom flask containing 100 mL of THF. *n*-Butyllithium (1.60 M, 18.7 mL, 29.9 mmol) was then added dropwise at −78 °C. After the reaction mixture was warmed to room temperature, a white precipitate formed. The flask was stirred at room temperature for 30 min, and then $C_6H_5SiMe_2Cl$ (5.16 g, 29.9 mmol) was added. The precipitate dissolved gradually, yielding a clear solution of the alkyne $PhMe_2SiC$≡CMe. The volatile materials were removed under vacuum, and then Cp_2ZrCl_2 (4.42 g, 15.1 mmol) and 70 mL of THF were added. The flask was cooled to −78 °C and 1.60 M *n*-butyllithium (18.7 mL, 29.9 mmol) was then added dropwise. The reaction mixture was warmed to room temperature and stirred overnight. All the volatile materials were removed in vacuo, and the residue was extracted into pentane (5 × 50 mL). Concentration (to 100 mL) and cooling the pentane solution (−40 °C) gave the product in 85% yield (7.3 g). ^{1}H NMR (benzene-d_6, 300 MHz): δ 7.74 (m, 4 H, C_6H_5), 7.30 (m, 4 H, C_6H_5,), 7.22 (m, 2 H, C_6H_5), 6.06 (s, 10 H, C_5H_5), 1.74 (s, 6 H, C_4Me_2), 0.29 (s, 12 H, SiMe_2Ph). $^{13}C\{^1H\}$ NMR (benzene-d_6, 100.6 MHz): δ 199.11 (ZrC_4Me_2), 149.45 (ZrC_4Me_2), 142.69 (C_6H_4, C), 134.23 (C_6H_4, CH), 128.61 (C_6H_4, CH), 128.20 (C_6H_4, CH), 111.47 (C_5H_5), 27.38 (ZrC_4Me_2), 2.07 (SiMe_2Ph). UV−vis (THF, nm): 214, 324. Anal. Calcd for $C_{32}H_{38}Si_2Zr$: C, 67.43; H, 6.72. Found: C, 67.26; H, 6.67.

$PhMe_2SiCH{=}CMeCMe{=}CHSiMe_2Ph$ (9). A 100 mL round-bottom flask was charged with **8** (0.50 g, 0.88 mmol) and THF (20 mL). An aqueous HCl solution (6 M, 20 mL) was added to the flask and the resulting mixture was stirred for 2 h at room temperature. The reaction solution was then extracted with pentane (2 × 20 mL), and a white solid was obtained by evaporation of pentane from the combined extracts. Recrystallization from methanol gave 0.27 g (87%) of the product as white plates. ^{1}H NMR (benzene-d_6, 300 MHz): δ 7.56 (m, 4 H, C_6H_5,), 7.22 (m, 4 H, C_6H_5), 7.20 (m, 2 H, C_6H_5), 6.00 (s, 2 H, $C_4Me_2H_2$), 1.94 (s, 6 H, C_4Me_2), 0.39 (s, 12 H, SiMe_2Ph). $^{13}C\{^1H\}$ NMR (benzene-d_6, 100.6 MHz): δ 155.88 ($C_4Me_2H_2$, C), 139.68 (C_6H_4, C), 134.13 (C_6H_4, CH), 129.16 (C_6H_4, CH), 128.20 (C_6H_4, CH), 124.41 ($C_4Me_2H_2$, CH), 20.65 ($C_4Me_2H_2$), −0.798 (SiMe_2Ph). UV−vis (THF, nm): 214, 260. mp 43−45 °C. EIMS: M$^+$ = 350. HRMS calcd for $C_{22}H_{30}Si_2$, 350.188608; found, 350.189125.

$PhMe_2SiC(I){=}CMeCMe{=}C(I)SiMe_2Ph$ (10). A 100 mL round-bottom flask was charged with **8** (1.00 g, 1.75 mmol), I_2 (0.95 g, 3.74 mmol), and THF (20 mL). The resulting red solution was stirred for 12 h, the THF was removed by vacuum transfer, and the resulting residue was extracted into pentane (3 × 20 mL). The pentane solution was washed with saturated $Na_2S_2O_3$ solution until colorless and then dried over Na_2SO_4. Pentane was removed to give 0.73 g (69%) of the product as a pale yellow oil. ^1H NMR (benzene-d_6, 300 MHz): δ 7.61 (m, 4 H, C_6H_5,), 7.19 (m, 4 H, C_6H_5), 7.17 (m, 2 H, C_6H_5), 1.71 (s, 6 H, C_4Me_2), 0.58 (s, 6 H, $SiMe_2Ph$), 0.52 (s, 6 H, $SiMe_2Ph$). $^{13}C\{^1H\}$ NMR (benzene-d_6, 100.6 MHz): δ 164.22 ($C_4Me_2I_2$), 138.26 (C_6H_4, C), 133.84 (C_6H_4, CH), 129.61 (C_6H_4, CH), 128.30 (C_6H_4, CH), 100.45 ($C_4Me_2I_2$), 20.19 ($C_4Me_2I_2$), 1.30 ($SiMe_2Ph$), 0.73 ($SiMe_2Ph$). EIMS: $M^+ - I^-$ (475) and $M^+ - 2I^-$ (348) were observed as the most intense peaks. The isotope pattern for these peaks were in good agreement with those obtained from simulation.

$[1,4\text{-}Me_2SiC_6H_4SiMe_2C_4Me_2H_2]_n$ (11). A 100 mL round-bottom flask was charged with **5** (0.95 g, 1.93 mmol) and THF (20 mL). An aqueous HCl solution (6 M, 20 mL) was added to the flask, and then the resulting mixture was stirred for 2 h at room temperature. The reaction mixture was poured into 200 mL of methanol, and the white precipitate was collected to afford 0.52 g (98%) of **11** as a white powder. ^1H NMR (benzene-d_6, 300 MHz): δ 7.62 (s, 4 H, C_6H_4), 6.02 (s, 2 H, $C_4Me_2H_2$), 1.96 (s, 6 H, C_4Me_2), 0.42 (s, 12 H, $SiMe_2$). $^{13}C\{^1H\}$ NMR (benzene-d_6, 100.6 MHz): δ 155.88 ($C_4Me_2H_2$, C), 140.35 (C_6H_4, C), 133.67 (C_6H_4, C), 124.39 ($C_4Me_2H_2$, CH), 20.76 ($C_4Me_2H_2$), −0.78 ($SiMe_2$). $M_n = 4200$, $M_w = 12\,000$. UV−vis (THF, nm): 232, 262. Anal. Calcd for $C_{16}H_{24}Si$: C, 70.51; H, 8.88. Found: C, 69.26; H, 8.99.

$[1,3\text{-}Me_2SiC_6H_4SiMe_2C_4Me_2H_2]_n$ (12). The method for **11** was followed (using **6**), to afford 0.38 g (70%) of **12** as a gummy solid. ^1H NMR (benzene-d_6, 400 MHz): δ 8.06 (s, 1 H, C_6H_4), 7.61 (d, $J = 7.6$, 2 H, C_6H_4), 7.29 (t, $J = 7.6$, 1 H, C_6H_4), 6.03 (s, 2 H, $C_4Me_2H_2$), 1.98 (s, 6 H, C_4Me_2), 0.45 (s, 12 H, $SiMe_2$). $^{13}C\{^1H\}$ NMR (benzene-d_6, 100.6 MHz): δ 155.88 ($C_4Me_2H_2$, C), 140.35 (C_6H_4, C), 133.67 (C_6H_4, C), 124.39 ($C_4Me_2H_2$, CH), 20.76 ($C_4Me_2H_2$), −0.780 ($SiMe_2$). $M_n = 1700$, $M_w = 3500$. Anal. Calcd for $C_{14}H_{24}Si_2$: C, 70.51; H, 8.88. Found: C, 61.77; H, 8.30.

$[4,4'\text{-}Me_2SiC_6H_4C_6H_4SiMe_2C_4Me_2H_2]_n$ (13). The method for **11** was followed (using **7**) to afford 0.56 g (91%) of **13** as a white powder. ^1H NMR (benzene-d_6, 400 MHz): δ 7.66 (d, $J = 8.0$, 4 H, C_6H_4), 7.61 (d, $J = 8.0$, 4 H, C_6H_4), 6.08 (s, 2 H, $C_4Me_2H_2$), 2.03 (s, 6 H, C_4Me_2), 0.46 (s, 12 H, $SiMe_2$). $^{13}C\{^1H\}$ NMR (benzene-d_6, 100.6 MHz): δ 155.98 ($C_4Me_2H_2$, C), 142.18 (C_6H_4, C), 138.57 (C_6H_4, C), 134.78 (C_6H_4, CH), 127.04 (C_6H_4, CH), 124.48 ($C_4Me_2H_2$, CH), 20.76 ($C_4Me_2H_2$), −0.72 ($SiMe_2$). $M_n = 6200$, $M_w = 13\,000$. Anal. Calcd for $C_{22}H_{28}Si_2$: C, 75.79; H, 8.09. Found: C, 74.80; H, 8.11.

$[1,4\text{-}Me_2SiC_6H_4SiMe_2C_4Me_2I_2]_n$ (14). A 100 mL round-bottom flask was charged with **5** (0.95 g, 1.93 mmol), I_2 (1.00 g, 3.94 mmol), and THF (20 mL). The resulting red solution was stirred for 12 h, and then the reaction mixture was poured into 200 mL of methanol. The resulting precipitate was collected to afford 0.75 g (74%) of **14** as a gray powder. ^1H NMR (benzene-d_6, 300 MHz): δ 7.71 (s, 4 H, C_6H_4), 1.73 (s, 6 H, C_4Me_2), 0.60 (s, 6 H, $SiMe_2$), 0.53 (s, 6 H, $SiMe_2$). ^{13}C NMR$\{^1H\}$ (benzene-d_6, 100.6 MHz): δ 164.31 ($C_4Me_2I_2$), 139.62 (C_6H_4, C), 133.84 (C_6H_4, CH), 100.31 ($C_4Me_2I_2$), 20.31 ($C_4Me_2I_2$), 1.12 ($SiMe_2$), 0.99 ($SiMe_2$), 0.79 ($SiMe_2$). $M_n = 5000$, $M_w = 8800$. UV−vis (THF, nm): 214, 233. Anal. Calcd for $C_{12}H_{22}Si_2I_2$: C, 36.65; H, 4.23; I, 48.41. Found: C, 36.74; H, 4.28; I, 48.22.

$[1,4\text{-}Me_2SiC_6H_4SiMe_2C_4Me_2ZrCp_2]_3$ (15). A 100 mL THF solution of polymer **5** (5.21 g) was heated at reflux for 24 h, and then the solution was concentrated to 30 mL and added to 70 mL of diethyl ether. The resulting solution was cooled to −20 °C to give the product as yellow cubic crystals in 93% yield (4.82 g). The compound was recrystallized from a THF/diethyl ether solution containing a slight amount of benzene. ^1H NMR (benzene-d_6, 300 MHz): δ 7.87 (s, 4 H, C_6H_4), 6.09 (s, 10 H, C_5H_5), 1.79 (s, 6 H, C_4Me_2), 0.31 (s, 12 H, $SiMe_2$). $^{13}C\{^1H\}$ NMR (benzene-d_6, 100.6 MHz): δ 198.93 (ZrC_4Me_2), 149.88 (ZrC_4Me_2), 142.82 (C_6H_4, C), 133.76 (C_6H_4, CH), 111.51 (C_5H_5), 27.68 (ZrC_4Me_2), 1.35 ($SiMe_2$). $M_n = 4600$, $M_w = 13\,000$. UV−vis (THF, nm): 214, 226, 326. Anal. Calcd for $C_{78}H_{96}Si_6Zr_3$ (not including the trapped benzene molecule): C, 63.48; H, 6.56. Found: C, 60.70; H, 6.93. EIMS: (no parent peak M^+ at 1470), $m/z = 765$ and 710 as the highest-mass peaks, assignable to the fragments $MeC{\equiv}CMe_2SiC_6H_4SiMe_2(C_4Me_2ZrCp_2){-}SiMe_2C_6H_4SiMe_2C{\equiv}CMe$ and $(Cp_2Zr)MeC{\equiv}CMe_2Si{-}C_6H_4SiMe_2C{\equiv}CMe(ZrCp_2)$. The isotope pattern for these peaks were successfully simulated.

$[1,4\text{-}Me_2SiC_6H_4SiMe_2C_4Me_2H_2]_3$ (16). A 100 mL round-bottom flask was charged with **15** (0.95 g, 1.93 mmol) and THF (20 mL). An aqueous HCl solution (6 M, 20 mL) was added to the flask, and the resulting mixture was stirred for 2 h at room temperature. This mixture was poured into 200 mL of methanol, and the white precipitate was collected to afford 0.52 g (98%) of **16** as a white powder. ^1H NMR (benzene-d_6, 300 MHz): δ 7.62 (s, 4 H, C_6H_4), 6.03 (s, 2 H, $C_4Me_2H_2$), 1.97 (s, 6 H, C_4Me_2), 0.43 (s, 12 H, $SiMe_2$). $^{13}C\{^1H\}$ NMR (benzene-d_6, 100.6 MHz): δ 155.88 ($C_4Me_2H_2$, C), 140.31 (C_6H_4, C), 133.67 (C_6H_4, CH), 124.27 ($C_4Me_2H_2$, CH), 20.76 ($C_4Me_2H_2$), −0.74 ($SiCH_2$). UV−vis (THF, nm): 232, 254. Anal. Calcd for $C_{48}H_{72}Si_6$: C, 70.51; H, 8.88. Found: C, 70.70; H, 10.03. EIMS showed $M^+ = 816$. HRMS calcd for $C_{48}H_{72}Si_6$, 816.424973; found, 816.425052.

$[1,4\text{-}Me_2SiC_6H_4SiMe_2C_4Me_2I_2]_3$ (17). A 100 mL round-bottom flask was charged with **15** (0.951 g, 1.93 mmol), I_2 (1.00 g, 3.94 mmol), and THF (20 mL). The resulting red solution was stirred for 12 h, and then the reaction mixture was poured into 200 mL of methanol. The precipitate was collected to afford 0.75 g (74%) of **17** as white crystals. ^1H NMR (benzene-d_6, 500 MHz): δ 7.601, 7.592, 7.590, 7.586 (4 singlets, 4 H, C_6H_4); 1.628, 1.604, 1.602, 1.573 (4 singlets, 6 H, C_4Me_2); 0.601, 0.599, 0.593, 0.588, 0.586 (overlapped singlets, 12 H, $SiMe_2$). ^{13}C NMR$\{^1H\}$ (benzene-d_6, 100.6 MHz): δ 164.24, 164.13, 164.06 (overlapped singlets, $C_4Me_2I_2$); 139.74, 139.67 (overlapped singlets, C_6H_4, C); 133.82, 133.80, 133.73 (overlapped singlets, C_6H_4, CH); 100.60, 100.47, 100.07, 100.00 (4 singlets, $C_4Me_2I_2$); 20.22, 20.18, 20.08, 20.05 (4 singlets, $C_4Me_2I_2$); 2.82, 2.78, 1.71, 1.69, −0.17, −0.32, −1.06, −1.08 (8 singlets, $SiCH_2$). UV−vis (THF, nm): 233, 280. Anal. Calcd for $C_{48}H_{66}Si_6I_6$: C, 36.65; H, 4.23. Found: C, 37.35; H, 4.45. EIMS showed the most intense peaks at $M^+ - 127\ (I^-) = 1445$; $M^+ - 254\ (2I^-) = 1318$; $M^+ - 381\ (3I^-) = 1191$; $M^+ - 508\ (4I^-) = 1064$; $M^+ - 635\ (5I^-) = 937$. The isotope pattern for these peaks was in good agreement with that obtained from simulation.

$[1,3\text{-}Me_2SiC_6H_4SiMe_2C_4Me_2ZrCp_2]_2$ (18). A 20 mL THF solution of polymer **6** (1.0 g) was heated in a thick-wall glass reactor at 80 °C for 24 h. During this period, yellow crystals precipitated from solution. Pentane (10 mL) was added to the reaction mixture, and the supernatant was filtered away to give **18** as yellow crystals in 85% yield (0.85 g). ^1H NMR (toluene-d_8, 400 MHz, 110 °C): δ 8.20 (s, 2 H, C_6H_4), 7.56 (d, $J_{HH} = 7.6$ Hz, 4 H, C_6H_4), 7.34 (t, $J_{HH} = 7.6$ Hz, 2 H, C_6H_4), 6.10 (s, 10 H, C_5H_5), 6.11 (s, 10 H, C_5H_5), 1.92 (s, 12 H, C_4Me_2), 0.52 (s, 12 H, $SiMe_2$), 0.04 (s, 12 H, $SiMe_2$). Due to its low solubility, a $^{13}C\{^1H\}$ NMR spectrum was not recorded. Anal. Calcd for $C_{52}H_{64}Si_4Zr_2$: C, 63.48; H, 6.56. Found: C, 63.44; H, 6.51.

$[1,3\text{-}Me_2SiC_6H_4SiMe_2C_4Me_2H_2]_2$ (19). A 100 mL round-bottom flask was charged with **18** (0.50 g, 1.0 mmol) and THF (20 mL). An aqueous HCl solution (6 M, 20 mL) was added to the flask, and then the resulting mixture was stirred for 2 h at room temperature. The yellow crystals of **18** dissolved, and a colorless solution formed. This solution was poured into 100 mL of methanol, and the white precipitate was collected to afford 0.20 g (72%) of **19** as a white powder. ^1H NMR (benzene-d_6, 400 MHz): δ 8.02 (s, 2 H, C_6H_4), 7.54 (d, $J_{HH} = 7.2$ Hz, 4 H, C_6H_4), 7.33 (t, $J_{HH} = 7.2$ Hz, 2 H, C_6H_4), 5.98 (s, 4 H, $C_4Me_2H_2$), 1.94 (s, 12 H, C_4Me_2), 0.36 (s, 24 H, $SiMe_2$). $^{13}C\{^1H\}$ NMR (benzene-d_6, 100.6 MHz): δ 156.15 ($C_4Me_2H_2$, C), 140.61 (C_6H_4, C), 138.74, 134.41 (C_6H_4, CH), 124.92 ($C_4Me_2H_2$, CH), 123.71, 21.06 ($C_4Me_2H_2$), −0.37 ($SiCH_3$). EIMS showed $M^+ = 544$. HRMS calcd for $C_{32}H_{48}Si_4$, 544.283316; found, 544.282772.

$[Me_2SiC_6H_4SiMe_2C_6H_4SiMe_2C_4Me_2ZrCp_2]_2$ (20). A 250 mL Schlenk flask was charged with Cp_2ZrCl_2 (0.58 g, 2.00 mmol), **4** (0.81 g, 2.00 mmol), and THF (80 mL). The flask was cooled to −78 °C, and then *n*-butyllithium (1.6 M/hexane, 2.50 mL, 4.00 mmol) was added dropwise. The flask was allowed to warm to room temperature over 7 h, and it was heated for 1 h at 65 °C. The volatile materials were removed under vacuum. The resulting residue was extracted with a mixture of dichloromethane and hexane (5:1, 80 mL), and the extract solution was then concentrated to 30 mL. A yellow crystalline solid (1.02 g, 82% yield) was isolated after cooling to −38 °C. ^{1}H NMR ($CDCl_3$, 400 Hz): δ 7.64 (dd, J_{HH} = 7 Hz, 8 H, C_6H_4), 6.27 (s, 10 H, C_5H_5), 1.66 (s, 6 H, C_4Me_2), 0.59 (s, 6 H, $SiMe_2$), 0.28 (s, 12 H, $C_4Me_2SiMe_2$). $^{13}C\{^1H\}$ NMR ($CDCl_3$, 100.6 Hz): δ 198.50 (ZrC_4Me_2, CZr), 148.91 (C_4Me_2, C), 143.25, 138.00 (C_6H_4, C), 133.47, 133.19 (C_6H_4, CH), 111.16 (C_5H_5), 27.24 (ZrC_4Me_2), 1.69 ($C_4Me_2SiMe_2$), −2.10 ($SiMe_2$). Anal. Calcd for $C_{68}H_{84}Si_6Zr_2$: C, 65.22; H, 6.76. Found: C, 65.08; H, 6.47.

$[Me_2SiC_6H_4SiMe_2C_6H_4SiMe_2C_4Me_2H_2]_2$ (21). This compound was prepared as a white solid in 96% yield from hydrolysis of **20**, following a procedure similar to that for **16**. ^{1}H NMR ($CDCl_3$, 400 Hz): δ 7.51 (dd, J_{HH} = 7.4 Hz, 8 H, C_6H_4), 5.82 (s, 2 H, $C_4Me_2H_2$), 2.11 (s, 6 H, C_4Me_2), 0.54 (s, 6 H, $C_4Me_2SiMe_2$), 0.39 (s, 12 H, $SiMe_2$). $^{13}C\{^1H\}$ NMR ($CDCl_3$, 100.6 Hz): δ 155.14 (C_4Me_2, C), 140.45, 138.52 (C_6H_4, C), 133.44, 133.06 (C_6H_4, CH), 124.04 ($C_4Me_2H_2$, CH), 20.18 (C_4Me_2), −1.03 ($C_4Me_2SiMe_2$), −2.47 ($SiMe_2$). EIMS showed M^+ = 812. HRMS calcd for $C_{48}H_{68}Si_6$, 812.393673; found: 812.392629. Anal. Calcd for $C_{48}H_{68}Si_6$: C, 70.86; H, 8.42. Found: C, 70.82; H, 8.21.

$[Me_2SiC_4Me_2ZrCp_2]_6$ (22). This compound was prepared by a procedure similar to that used for **6**, but with heating of the reaction solution to 65 °C for 3 h after warming to room temperature. The product precipitated from the reaction solution as a yellow solid, which was washed with THF (2 × 50 mL) to give an 72% yield after filtration. Due to its very poor solubility, ^{1}H and ^{13}C NMR spectra were not recorded. Anal. Calcd for $C_{108}H_{132}Si_6Zr_6$: C, 60.44; H, 6.20. Found: C, 60.28; H, 6.02.

$[Me_2SiC_4Me_2H_2]_6$ (23). This compound was prepared as a white solid in 95% yield via hydrolysis of **22** following a procedure similar to that for **16**. ^{1}H NMR ($CDCl_3$, 500 Hz): δ 5.77 (s, 2H, $C_4H_2Me_2$) 1.97 (s, 6 H, C_4Me_2), 0.27 (s, 6H, $SiMe_2$). $^{13}C\{^1H\}$ NMR ($CDCl_3$, 125 Hz): δ 153.85 ($C_4Me_2H_2$, C), 125.78 ($C_4Me_2H_2$, CH), 20.10 ($C_4Me_2H_2$), −0.06 ($SiMe_2$). EIMS showed M^+ = 828.6. HRMS calcd for $C_{48}H_{84}Si_6$, 828.518874; found: 828.520059. Anal. Calcd for $C_{48}H_{84}Si_6$: C, 69.49; H, 10.20. Found: C, 69.12; H, 10.18.

[4,4′-$Me_2SiC_6H_4C_6H_4SiMe_2C_4Me_2ZrCp_2]_3$ (24). An 80 mL THF solution of polymer **7** (0.50 g) was heated in a thick-wall flask to 80 °C for 16 h. The solution was then concentrated to 10 mL and added to 70 mL of pentane. The resulting yellow solid was collected to give the product in 90% yield (0.45 g). ^{1}H NMR (benzene-d_6, 400 MHz): δ 7.84 (d, J_{HH} = 8.0 Hz, 4 H, C_6H_4), 7.76 (d, J_{HH} = 8.0 Hz, 4 H, C_6H_4), 6.13 (s, 10 H, C_5H_5), 1.78 (s, 6 H, C_4Me_2), 0.34 (s, 12 H, $SiMe_2$). $^{13}C\{^1H\}$ NMR (benzene-d_6, 100.6 MHz): δ 199.41 (ZrC_4Me_2), 149.61 (ZrC_4Me_2), 141.76 (C_6H_4, C), 141.46 (C_6H_4, C), 134.82 (C_6H_4, CH), 126.89 (C_6H_4, CH), 111.52 (C_5H_5), 27.54 (ZrC_4Me_2), 2.17 ($SiMe_2$). M_n = 1440, M_w = 1442 (GPC). Anal. Calcd for $C_{32}H_{36}Si_2Zr$: C, 67.66; H, 6.39. Found: C, 67.84; H, 6.04. By GPC, this yellow powder contains 90% of **24** and 10% of polymer **7**.

[4,4′-$Me_2SiC_6H_4C_6H_4SiMe_2C_4Me_2H_2]_3$ (25). A THF solution (5 mL) of **24** (0.20 g, 0.12 mmol) and an aqueous HCl solution (5 mL, 6 M) were added to a flask, and then the resulting mixture was stirred for 2 h at room temperature. All volatile materials were removed from this mixture in vacuo, and the residue was extracted with pentane (2 × 10 mL). Removal of pentane from the extracts afforded 0.10 g (80%) of **25** as a white solid. ^{1}H NMR (benzene-d_6, 400 MHz): δ 7.58 (m, 8H, $C_6H_4{-}C_6H_4$), 6.06 (s, 2 H, $C_4Me_2H_2$), 2.03 (s, 6 H, C_4Me_2), 0.46 (s, 12 H, $SiMe_2$). $^{13}C\{^1H\}$ NMR (benzene-d_6, 100.6 MHz): δ 155.80 ($C_4Me_2H_2$, C), 142.15 (C_6H_4, C), 138.49 (C_6H_4, C), 134.79 (C_6H_4, CH), 134.03 (C_6H_4, C), 127.76 (C_6H_4, CH), 124.36 ($C_4Me_2H_2$, CH), 20.76 ($C_4Me_2H_2$), −0.72 ($SiMe_2$). EIMS showed M^+ = 1046. The isotope pattern for these peaks was in good agreement with that obtained from simulation. HRMS calcd for $C_{66}H_{84}Si_6$: 1044.518874, found: 1044.519160.

Crystallographic Structure Determination of 15. Cracked yellowish blocky crystals of **15** were obtained by slow crystallization from a THF solution of **15** containing a trace amount of benzene. Fragments cleaved from some of these crystals were mounted on glass fibers using Paratone N hydrocarbon oil. The crystals were then transferred to an Enraf-Nonius CAD-4 diffractometer and centered in the beam. They were cooled to −86 °C by a nitrogen flow low-temperature apparatus which had been previously calibrated by a thermocouple placed at the sample position. Automatic peak search and indexing procedures yielded a monoclinic reduced primitive cell. The 12 206 raw intensity data were converted to structure factor amplitudes and their esds by correction for scan speed, background, and Lorentz and polarization effects. No correction for crystal decomposition was necessary. An empirical correction was made to the data based on the combined differences of F_{obs} and F_{clc} following refinement of all atoms with isotropic thermal parameters (T_{max} = 1.03, T_{min} = 0.94). Inspection of the systematic absences indicated uniquely space group $P2_1/n$. Removal of systematically absent data left 11 755 unique data in the final data set. The structure was solved by Patterson methods and refined via standard least-squares and Fourier techniques. Following location of the Zr atoms and the ligands, four areas of electron density were discovered, presumed to be a benzene molecule. The first two areas were modeled with full-occupancy carbon atoms. The other two were modeled with partial occupancy carbon atoms refined with a common isotropic thermal parameter. Partial atoms were added as long as the area modeled remained compact. Partial atoms were removed when their occupancies fell below 0.2. The solvent was assumed to be benzene in reporting the empirical formula and density. Hydrogen atoms for the ligand were assigned idealized locations and values of B_{iso} approximately 1.25 times the B_{eqv} of the atoms to which they were attached. They were included in structure factor calculations but not refined. In the final cycles of least-squares 3 data with abnormally large weighted difference values were given zero weight. One carbon atom in the trimeric ligand (C61) refused to refine correctly with anisotropic thermal parameters and was refined with an isotropic thermal parameter in the final cycles. The final residuals for 899 variables refined against the 5520 accepted data for which $F^2 > 3s(F^2)$ were R = 5.29%, wR = 5.46%, and GOF = 1.28. The R value for all 11 755 data was 14.5%.

Crystallographic Structure Determination of 16. Clear, colorless, bladelike crystals of **16** were obtained by slow crystallization from acetonitrile. A fragment cut from one of these crystals was mounted on a glass fiber using Paratone N hydrocarbon oil. The crystal was then transferred to a Enraf-Nonius CAD-4 diffractometer and centered in the beam. It was cooled to −128 °C by a nitrogen flow low temperature apparatus which had been previously calibrated by a thermocouple placed at the sample position. Automatic peak search and indexing procedures yielded a monoclinic reduced primitive cell. The 3577 raw intensity data were converted to structure factor amplitudes and their esds by correction for scan speed, background, and Lorentz and polarization effects. No correction for crystal decomposition was necessary, and no correction for absorption was applied. Inspection of the systematic absences indicated uniquely space group $P2_1/c$. Removal of systematically absent data left 3313 unique data in the final data set. The structure was solved by direct methods in space groups $P2_1$ and Pc, to show the trimeric molecule, and the near-exact relationship of the Si atoms to symmetrically equivalent positions was observed in the centric space group $P2_1/c$. Wilson statistics clearly indicated the centric space group and refinement in the acentric space groups did not converge readily and continually indicated overlap of phenyl and dienyl fragments between each pair of Si atoms. The final model in the centric space group has ordered Si and Si-methyl carbons refined with anisotropic thermal parameters and all other carbon atoms with occupancy factors of 0.50 and isotropic thermal parameters. The final residuals for 226 variables refined against the 1648 data for which $F^2 > 3s(F^2)$ were R = 9.77%, wR = 12.2%, and GOF = 2.85. The R value for all 3313 data was 17.9%.

Crystallographic Structure Determination of 18. Yellow, cubic crystals of **18** were obtained by slow cooling of a THF solution from 60 °C to room temperature. A fragment cut from one of these crystals with a dimension of 0.2 × 0.15 × 0.1 mm was mounted on a glass fiber using Paratone N hydrocarbon oil. The crystal was then transferred to a SMART diffractometer with graphite monochromated Mo−Kα radiation and centered in the beam. It was cooled to −160 °C by a nitrogen flow low temperature apparatus which had been previously calibrated by a thermocouple placed at the sample position. Automatic peak search and indexing procedures yielded a triclinic reduced primitive cell. No correction for crystal decomposition was necessary, and no correction for absorption was applied. Inspection of the systematic absences indicated uniquely space group $P2_1/c$. The structure was solved by direct methods in space group P and expanded using Fourier techniques. All non-hydrogen atoms were refined with anisotropic thermal parameters. Hydrogen atoms were refined isotropically. All calcu-lations were performed using the teXsan crystallographic software package of Molecular Structure Corporation. The final residuals for 444 variables refined against the 3495 data for which $I > 3.00\sigma(I)$ were $R = 3.9\%$, $wR = 5.3\%$, and GOF = 2.17.

Acknowledgment is made to the National Science Foundation for their generous support of this work. We also thank Dr. Fred Hollander for assistance with the X-ray structure determinations.

Supporting Information Available: Tables of crystal, data collection, and refinement parameters, bond distances and angles, and anisotropic displacement parameters for **15**, **16**, and **18** (29 pages). See any current masthead page for ordering and Internet access instructions.

JA973180U